28: 1454–1460.
22. Liu W, Hu D, Li C, Li P, Li Y, Li Z, et al. Mutation analysis of potassium channel genes KCNQ1 and KCNH2 in patients with long QT syndrome. *Chin Med J (Engl)* 2003; **116:** 1333–1335.
23. Gray C, Gula LJ, Klein GJ, Skanes AC, Yee R, Sy R, et al. Expression of a common LQT1 mutation in five apparently unrelated families in a regional inherited arrhythmia clinic. *J Cardiovasc Electrophysiol* 2010; **21:** 296–300.
24. Fodstad H, Swan H, Laitinen P, Piippo K, Paavonen K, Viitasalo M, et al. Four potassium channel mutations account for 73% of the genetic spectrum underlying long-QT syndrome (LQTS) and provide evidence for a strong founder effect in Finland. *Ann Med* 2004; **36:** 53–63.
25. Piippo K, Swan H, Pasternack M, Chapman H, Paavonen K, Viitasalo M, et al. A founder mutation of the potassium channel KCNQ1 in long QT syndrome: Implications for estimation of disease prevalence and molecular diagnostics. *J Am Coll Cardiol* 2001; **37:** 562–568.
26. Postema PG, Van den Berg M, Van Tintelen JP, Van den Heuvel F, Grundeken M, Hofman N, et al. Founder mutations in the Netherlands: SCN5a 1795insD, the first described arrhythmia overlap syndrome and one of the largest and best characterized families worldwide. *Neth Heart J* 2009; **17:** 422–428.
27. Zareba W, Moss AJ, Schwartz PJ, Vincent GM, Robinson JL, Priori SG, et al. Influence of genotype on the clinical course of the long-QT syndrome: International Long-QT Syndrome Registry Research Group. *N Engl J Med* 1998; **339:** 960–965.
28. Beaufort-Krol GC, van den Berg MP, Wilde AA, van Tintelen JP, Viersma JW, Bezzina CR, et al. Developmental aspects of long QT syndrome type 3 and Brugada syndrome on the basis of a single SCN5A mutation in childhood. *J Am Coll Cardiol* 2005; **46:** 331–337.
29. Schwartz PJ, Spazzolini C, Crotti L. All LQT3 patients need an ICD: True or false? *Heart Rhythm* 2009; **6:** 113–120.
30. Schwartz PJ, Priori SG, Locati EH, Napolitano C, Cantù F, Towbin JA, et al. Long QT syndrome patients with mutations of the SCN5A and HERG genes have differential responses to Na^+ channel blockade and to increases in heart rate: Implications for gene-specific therapy. *Circulation* 1995; **92:** 3381–3386.
31. Shimizu W, Antzelevitch C. Sodium channel block with mexiletine is effective in reducing dispersion of repolarization and preventing torsade des pointes in LQT2 and LQT3 models of the long-QT syndrome. *Circulation* 1997; **96:** 2038–2047.
32. Ruan Y, Liu N, Bloise R, Napolitano C, Priori SG. Gating properties of SCN5A mutations and the response to mexiletine in long-QT syndrome type 3 patients. *Circulation* 2007; **116:** 1137–1144.
33. Ruan Y, Denegri M, Liu N, Bachetti T, Seregni M, Morotti S, et al. Trafficking defects and gating abnormalities of a novel SCN5A mutation question gene-specific therapy in long QT syndrome type 3. *Circ Res* 2010; **106:** 1374–1383.

JOURNAL OF THE AMERICAN COLLEGE OF CARDIOLOGY
© 2014 BY THE AMERICAN COLLEGE OF CARDIOLOGY FOUNDATION
PUBLISHED BY ELSEVIER INC.

VOL. 64, NO. 1, 2014
ISSN 0735-1097/$36.00
http://dx.doi.org/10.1016/j.jacc.2014.04.023

EDITORIAL COMMENT

Importance of Clinical Analysis in the New Era of Molecular Genetic Screening*

Wataru Shimizu, MD, PHD

For the past 2 decades, a number of inherited cardiac arrhythmia syndromes have been shown to be linked to mutations in genes encoding cardiac ion channels or other membrane components. These include congenital and acquired long-QT syndrome (LQTS), Brugada syndrome (BrS), progressive cardiac conduction defect, catecholaminergic polymorphic ventricular tachycardia (CPVT), short-QT syndrome, early repolarization syndrome, and familial atrial fibrillation (AF) (1). In congenital LQTS, 13 genotypes have been identified in approximately 75% of subjects with clinically diagnosed congenital LQTS (1,2), and genotype-phenotype

SEE PAGE 66

correlations have been investigated in detail. Thus, genetic testing is now a gold standard for diagnosing congenital LQTS, enabling risk stratification of cardiac events and better patient management (1). Mutations in the *RyR2* gene or *calsequestrin* gene can be identified in approximately 60% of typical patients with CPVT associated with bidirectional and/or multifocal ventricular tachycardia (1,2). However, the yield associated with disease-specific genetic testing is far short of 100%, even in congenital LQTS or CPVT. Moreover, causative mutations have been identified in a small number of patients with other inherited arrhythmia syndromes (1). The yield of disease-specific genetic testing is only 20% to 30% in BrS and is still unknown in progressive cardiac conduction defect, short-QT syndrome, early repolarization syndrome, and familial AF (1,2).

In BrS, the first mutation was identified in an alpha subunit of a sodium channel gene, *SCN5A*, in 1998 (3). Subsequently, genetic studies have identified 13 responsible genes on chromosomes 1, 3, 7, 10, 11, 12, 17, and 19 (1). Among 13 genotypes, more than 300 mutations have been identified in the major player, *SCN5A* (>75% of genotyped cases); however, a worldwide cohort reported that *SCN5A* accounts only for 11% to 28% of clinically diagnosed patients with BrS (4). Moreover, the majority of mutations were found in a single family or a small number of families. Therefore, a genotype-phenotype correlation is not available in most cases (1,5).

The relatively lower yield of disease-specific genetic testing except for congenital LQTS or CPVT is due mainly to the technology of genetic testing. Candidate gene analysis has long been used to identify a causative mutation in a gene, which is expected to relate to the pathophysiology of each inherited arrhythmia syndrome, such as cardiac ion channel genes. However, causative mutations do not always involve genes of ion channels or membrane components. Innovative advances in molecular genetic testing are overcoming this issue with the advent of more powerful molecular genetic screening tools, including genome-wide association study (GWAS) using gene array, as well as targeted, whole-exome and whole-genome next-generation sequencing techniques.

Several recent GWASs have disclosed significant association of numerous loci in some genes with electrocardiographic markers or arrhythmia syndromes. Arking et al. (6) first identified *NOS1AP (CAPON)*, a regulator of neuronal nitric oxide synthase, as a gene that is significantly associated with QT-interval variation in a general population derived from 3 cohorts (6). Subsequently, 2 groups conducted a meta-analysis of the GWAS and observed associations

* Editorials published in the *Journal of the American College of Cardiology* reflect the views of the authors and do not necessarily represent the views of *JACC* or the American College of Cardiology.

From the Department of Cardiovascular Medicine, Nippon Medical School, Tokyo, Japan. Dr. Shimizu is supported in part by a Research Grant for the Cardiovascular Diseases (H24-033) from the Ministry of Health, Labour and Welfare, Japan.

of single-nucleotide polymorphisms (SNPs) in several genes in addition to *NOS1AP* with QT interval, suggesting that these genes are candidate genes for LQTS or sudden cardiac death (7,8). Several GWASs also identified associations of SNPs in several genes, including *SCN10A*, with cardiac conduction parameters, such as QRS duration and PR interval (9-11). Regarding associations with cardiac arrhythmias, some SNPs in several genes, including *ZFHX3* and *KCNN3*, have been reported to be associated with AF (12-14). The association of a SNP in *CXADR* with ventricular fibrillation in acute myocardial infarction also has been reported (15). However, no responsible mutations have thus far been reported in these candidate genes in patients with clinically diagnosed inherited arrhythmia syndromes, such as congenital LQTS, familial AF, and familial conduction abnormalities.

Bezzina et al. (16) recently conducted a GWAS in 312 patients with BrS with type 1 electrocardiographic pattern and 1,115 controls. They detected 2 significant association signals at the *SCN10A* intronic locus (rs10428132) in chromosome 3p22 and near the *HEY2* gene (rs9388451) in chromosome 6q22 with BrS. *SCN10A*, which encodes the sodium channel isoform Nav1.8, was originally reported as highly expressed in cardiac neurons. Recent evidence indicates that *SCN10A* also is expressed in the working myocardium and the specialized conduction system, indicating a possible role for Nav1.8 in cardiac electrical function. *HEY2* is involved in patterning Nav1.5 (*SCN5A*) expression across the ventricular wall. In an experiment using *HEY2* knockout mouse, Bezzina et al. (16) suggested that loss of *HEY2* might affect the transmural expression gradient of sodium channel implicated in BrS.

In this issue of the *Journal*, Hu et al. (17) report on a clinical analysis and direct sequencing of *SCN10A* and all known BrS genes in 150 unrelated patients with BrS and 17 family members, as well as more than 200 ethnically matched healthy controls. They identified 17 *SCN10A* mutations in 25 of 150 patients with BrS (a yield of 16.7%). Twenty-three of the 25 (92.0%) displayed overlapping phenotypes, such as early repolarization syndrome and cardiac conduction defect. Patients with BrS with *SCN10A* mutations were more symptomatic and displayed significantly longer PR and QRS intervals than *SCN10A*-negative patients with BrS. Heterologous coexpression of *SCN10A* mutants (R14L and R1268Q) with wild-type *SCN5A* caused 79.4% and 84.4% reductions in sodium channel current, strongly implicating *SCN10A* as a major susceptibility gene for BrS. This study provides the first major step forward in more than 16 years in the identification of new BrS susceptibility genes, advancing the yield for detection of a genotype to more than 50%.

New molecular genetic screening technologies, such as GWAS and whole-exome and whole-genome next-generation sequencing, are promising tools for identifying new candidate genes responsible for inherited arrhythmia syndromes. However, no responsible mutations have been reported in the candidate genes identified by GWAS in patients with clinically diagnosed inherited arrhythmia syndromes. To the best of my knowledge, the *SCN10A* is the first gene to be suggested as a BrS susceptibility gene by both GWAS and direct sequencing techniques. Direct sequencing using the Sanger technique combined with a detailed clinical analysis, including genotype-phenotype correlation and functional expression studies, continue to play an important role in molecular genetic testing, even in the new era in which gene arrays and next-generation sequencing are available. The importance of a detailed clinical analysis including genotype-phenotype correlation as well as functional expression studies cannot be overemphasized. Even in GWAS and whole-genome or whole-exome studies, clinical misdiagnosis can contribute to confounding genetic noise. A detailed, precise clinical diagnosis is therefore a prerequisite for the identification of new potential candidate genes.

REPRINT REQUESTS AND CORRESPONDENCE: Dr. Wataru Shimizu, Nippon Medical School, Department of Cardiovascular Medicine, 1-1-5, Sendagi Bunkyo-ku, Tokyo 113-8603, Japan. E-mail: wshimizu@nms.ac.jp.

REFERENCES

1. Shimizu W. Update of diagnosis and management in inherited cardiac arrhythmias. Circ J 2013; 77:2867-72.
2. Ackerman MJ, Priori SG, Willems S, et al. HRS/EHRA expert consensus statement on the state of genetic testing for the channelopathies and cardiomyopathies this document was developed as a partnership between the Heart Rhythm Society (HRS) and the European Heart Rhythm Association (EHRA). Heart Rhythm 2011;8:1308-39.
3. Chen Q, Kirsch GE, Zhang D, et al. Genetic basis and molecular mechanisms for idiopathic ventricular fibrillation. Nature 1998;392:293-6.
4. Kapplinger JD, Tester DJ, Alders M, et al. An international compendium of mutations in the SCN5A-encoded cardiac sodium channel in patients referred for Brugada syndrome genetic testing. Heart Rhythm 2010;7:33-46.
5. Shimizu W. Clinical features of Brugada syndrome. J Arrhythmia 2013;29:65-70.
6. Arking DE, Pfeufer A, Post W, et al. A common genetic variant in the NOS1 regulator NOS1AP modulates cardiac repolarization. Nat Genet 2006;38:644-51.

JACC VOL. 64, NO. 1, 2014
JULY 8, 2014:80-2

7. Newton-Cheh C, Eijgelsheim M, Rice KM, et al. Common variants at ten loci influence QT interval duration in the QTGEN Study. Nat Genet 2009;41:399-406.

8. Pfeufer A, Sanna S, Arking DE, et al. Common variants at ten loci modulate the QT interval duration in the QTSCD Study. Nat Genet 2009;41:407-14.

9. Chambers JC, Zhao J, Terracciano CM, et al. Genetic variation in SCN10A influences cardiac conduction. Nat Genet 2010;42:149-52.

10. Pfeufer A, van Noord C, Marciante KD, et al. Genome-wide association study of PR interval. Nat Genet 2010;42:153-9.

11. Sotoodehnia N, Isaacs A, de Bakker PI, et al. Common variants in 22 loci are associated with QRS duration and cardiac ventricular conduction. Nat Genet 2010;42:1068-76.

12. Benjamin EJ, Rice KM, Arking DE, et al. Variants in ZFHX3 are associated with atrial fibrillation in individuals of European ancestry. Nat Genet 2009;41:879-81.

13. Ellinor PT, Lunetta KL, Glazer NL, et al. Common variants in KCNN3 are associated with lone atrial fibrillation. Nat Genet 2010;42:240-4.

14. Ellinor PT, Lunetta KL, Albert CM, et al. Meta-analysis identifies six new susceptibility loci for atrial fibrillation. Nat Genet 2012;44:670-5.

15. Bezzina CR, Pazoki R, Bardai A, et al. Genome-wide association study identifies a susceptibility locus at 21q21 for ventricular fibrillation in acute myocardial infarction. Nat Genet 2010;42:688-91.

16. Bezzina CR, Barc J, Mizusawa Y, et al. Common variants at SCN5A-SCN10A and HEY2 are associated with Brugada syndrome, a rare disease with high risk of sudden cardiac death. Nat Genet 2013;45:1044-9.

17. Hu D, Barajas-Martínez H, Pfeiffer R, et al. Mutations in *SCN10A* are responsible for a large fraction of cases of Brugada syndrome. J Am Coll Cardiol 2014;64:66-79.

KEY WORDS Brugada syndrome, direct sequencing, genetic study, GWAS, sudden death

Cardiovascular Research (2014) **104**, 183–193
doi:10.1093/cvr/cvu185

Inhibition of N-type Ca^{2+} channels ameliorates an imbalance in cardiac autonomic nerve activity and prevents lethal arrhythmias in mice with heart failure

Yuko Yamada[1,2†], Hideyuki Kinoshita[1,3†], Koichiro Kuwahara[1,3*], Yasuaki Nakagawa[1,3], Yoshihiro Kuwabara[1,4], Takeya Minami[1,3], Chinatsu Yamada[1,3], Junko Shibata[1,3], Kazuhiro Nakao[1,2,3], Kosai Cho[3,5], Yuji Arai[6], Shinji Yasuno[4], Toshio Nishikimi[1,3], Kenji Ueshima[4], Shiro Kamakura[7], Motohiro Nishida[8], Shigeki Kiyonaka[9], Yasuo Mori[9], Takeshi Kimura[3], Kenji Kangawa[2,10], and Kazuwa Nakao[1,11]

[1]Department of Medicine and Clinical Science, Kyoto University Graduate School of Medicine, 54 Shogoin Kawaharacho, Sakyo-ku, Kyoto 606-8507, Japan; [2]Department of Peptide Research, Kyoto University Graduate School of Medicine, Kyoto 606-8507, Japan; [3]Department of Cardiovascular Medicine, Kyoto University Graduate School of Medicine, Kyoto 606-8507, Japan; [4]Department of EBM Research, Institute for Advanced of Clinical and Translational Science, Kyoto University Hospital, Kyoto 606-8507, Japan; [5]Department of Primary Care and Emergency Medicine, Kyoto University Graduate School of Medicine, Kyoto 606-8507, Japan; [6]Department of Bioscience and Genetics, National Cerebral and Cardiovascular Center Research Institute, Suita 565-8565, Japan; [7]Department of Cardiovascular Medicine, National Cerebral and Cardiovascular Center, Suita 565-8565, Japan; [8]Division of Cardiocirculatory Signaling, Okazaki Institute for Integrative Bioscience (National Institute for Physiological Sciences), National Institute for Natural Sciences, Aichi 444-8787, Japan; [9]Department of Synthetic Chemistry and Biological Chemistry, Kyoto University Graduated School of Engineering, Kyoto 615-8530, Japan; [10]Department of Biochemistry, National Cerebral and Cardiovascular Center Research Institute, Suita 606-8507, Japan; and [11]Medical Innovation Center, Kyoto University Graduate School of Medicine, Kyoto 606-8507, Japan

Received 21 January 2014; revised 24 July 2014; accepted 30 July 2014; online publish-ahead-of-print 5 August 2014

Time for primary review: 10 days

Aims Dysregulation of autonomic nervous system activity can trigger ventricular arrhythmias and sudden death in patients with heart failure. N-type Ca^{2+} channels (NCCs) play an important role in sympathetic nervous system activation by regulating the calcium entry that triggers release of neurotransmitters from peripheral sympathetic nerve terminals. We have investigated the ability of NCC blockade to prevent lethal arrhythmias associated with heart failure.

Methods and results We compared the effects of cilnidipine, a dual N- and L-type Ca^{2+} channel blocker, with those of nitrendipine, a selective L-type Ca^{2+} channel blocker, in transgenic mice expressing a cardiac-specific, dominant-negative form of neuron-restrictive silencer factor (dnNRSF-Tg). In this mouse model of dilated cardiomyopathy leading to sudden arrhythmic death, cardiac structure and function did not significantly differ among the control, cilnidipine, and nitrendipine groups. However, cilnidipine dramatically reduced arrhythmias in dnNRSF-Tg mice, significantly improving their survival rate and correcting the imbalance between cardiac sympathetic and parasympathetic nervous system activity. A β-blocker, bisoprolol, showed similar effects in these mice. Genetic titration of NCCs, achieved by crossing dnNRSF-Tg mice with mice lacking *CACNA1B*, which encodes the α1 subunit of NCCs, improved the survival rate. With restoration of cardiac autonomic balance, dnNRSF-Tg;*CACNA1B*$^{+/-}$ mice showed fewer malignant arrhythmias than dnNRSF-Tg;*CACNA1B*$^{+/+}$ mice.

Conclusions Both pharmacological blockade of NCCs and their genetic titration improved cardiac autonomic balance and prevented lethal arrhythmias in a mouse model of dilated cardiomyopathy and sudden arrhythmic death. Our findings suggest that NCC blockade is a potentially useful approach to preventing sudden death in patients with heart failure.

Keywords Ion channel • Nervous system • Autonomic • Heart failure • Arrhythmia • N-type Ca^{2+} channel

* Corresponding author. Tel: +81 75 751 4287; fax: +81 75 771 9452. E-mail: kuwa@kuhp.kyoto-u.ac.jp

† These authors contributed equally to this work.

1. Introduction

Approximately 50% of deaths among patients with heart failure are classified as sudden death, mainly caused by lethal arrhythmias.[1] Despite recent progress, pharmacological interventions for the treatment and prevention of lethal arrhythmias associated with chronic heart failure remain unsatisfactory. Nonetheless, it is anticipated that a better understanding of the molecular basis of arrhythmicity in failing hearts will enable identification of therapeutic targets that can serve as the basis for the development of new pharmacological treatments.

Autonomic dysregulation leading to increased sympathetic nerve activity and decreased parasympathetic nerve activity contributes to the increased arrhythmicity seen in patients with chronic heart failure.[2,3] N-type voltage-dependent Ca^{2+} channels (NCCs), encoded by the *CACNA1B* (α1B subunit) gene, are predominantly localized in the nervous system, where they play a pivotal role in modulating a variety of neuronal functions, including neurotransmitter release at sympathetic nerve terminals.[4–6] Mice lacking *CACNA1B* show functional deterioration of their sympathetic nervous system,[7] and the ability of NCC blockade to prevent malignant arrhythmias and sudden death associated with heart failure remains unevaluated.

We previously reported that transgenic mice cardiac-selectively expressing a dominant-negative form of neuron-restrictive silencer factor (NRSF, also called REST) (dnNRSF-Tg), a transcriptional repressor important for regulation of the fetal cardiac gene program, showed progressive cardiomyopathy and sudden arrhythmic death beginning at about 8 weeks of age.[8] We have also reported several abnormalities in cardiac electrophysiological properties and ion channel expression in these dnNRSF-Tg mice.[9,10] The dnNRSF-Tg hearts showed increased expression of fetal-type ion channel genes, including *CACNA1H*, which encodes the T-type Ca^{2+} channel (TCC) α1 subunit, and a corresponding increase in $I_{ca,T}$ amplitude.[8] In that earlier study, we demonstrated that TCC blockade could prevent sudden death in dnNRSF-Tg mice by both restoring the normal electrophysiology of ventricular myocytes and correcting the cardiac autonomic dysfunction observed in dnNRSF-Tg mice.[11] Because TCC expression, and thus functional TCC currents, is increased in the myocardium of dnNRSF-Tg mice, TCC blockade directly affects the electrophysiological properties of ventricular myocytes in dnNRSF-Tg mice. On the other hand, the impact of modulating autonomic nervous system balance on the incidence of lethal arrhythmias in dnNRSF-Tg mice remains unclear.

Pharmacological blockade or genetic deletion of NCCs reportedly alters autonomic activity in both human patients and animal models.[7,12,13] On the other hand, little or no NCC expression has been detected in the ventricular myocardium. Therefore, to evaluate the extent to which correcting the autonomic imbalance prevents the lethal arrhythmias associated with heart failure, we assessed the effects of pharmacological blockade of NCCs and their genetic titration on arrhythmicity and sudden death in dnNRSF-Tg mice. Our findings demonstrate the importance of an imbalance between sympathetic and parasympathetic nerve activities in the generation of lethal arrhythmias in failing hearts and suggest that restoring autonomic nervous system balance through NCC inhibition can be an effective approach to preventing sudden arrhythmic death associated with heart failure.

2. Methods

An expanded Methods section is available in Supplementary material online.

2.1 Animal experiments

The animal care and all experimental protocols were reviewed and approved by the Animal Research Committee at Kyoto University Graduate School of Medicine, and conformed to the US National Institute of Health Guide for the Care and Use of Laboratory Animals. Beginning at 8 weeks of age, dnNRSF-Tg mice were left untreated (control) or were treated for 24 weeks with cilnidipine (10 mg/kg/day po) or nitrendipine (10 mg/kg/day po). The drug dosages were chosen based on earlier reports and our preliminary studies.[14,15] Cilnidipine was supplied by Mochida Pharmaceutical Co., Ltd (Tokyo, Japan). Nitrendipine was purchased from Wako Pure Chemical Industries, Ltd (Osaka, Japan). Bisoprolol was supplied by Mitsubishi Tanabe Pharma Corporation (Osaka, Japan). Cilnidipine exerts a much more potent inhibitory effect on N-type Ca^{2+} currents than does nitrendipine, which has little effect on N-type Ca^{2+} currents, particularly under conditions in which L-type Ca^{2+} current inhibition is comparable between the two drugs.[16,17] We then selected the doses of both drugs that similarly and minimally affected blood pressure. In another experiment, dnNRSF-Tg mice were bred with *CACNA1B* heterozygous knockout mice to obtain dnNRSF-Tg; $CACNA1B^{+/-}$ mice and control dnNRSF-Tg;$CACNA1B^{+/+}$ littermates. $CACNA1B^{+/-}$ mice were described in an earlier report.[7] For the isolation and analysis of hearts, mice were anaesthetized with 3.0% of isoflurane and sacrificed by cervical dislocation.

2.2 Statistical analysis

Data are presented as means ± standard errors of the mean (SEM) unless indicated otherwise. Survival was analysed using the Kaplan–Meier method with the log-rank test. Comparisons among multiple groups were made using ANOVA with post hoc Fisher's tests, except for numbers of arrhythmias. Values of $P < 0.05$ were considered significant. Numbers of arrhythmias between two groups were analysed using the Mann–Whitney test. Values of $P < 0.05$ were considered significant. Numbers of arrhythmias among four groups were analysed using Kruskal–Wallis non-parametric ANOVA followed by the Bonferroni correction. Values of $P < 0.0083$ were considered significant in that analysis.

3. Results

3.1 The dual N- and L-type Ca^{2+} channel blocker cilnidipine improves survival among dnNRSF-Tg mice without affecting cardiac structure or function

We initially confirmed that there is little expression of *CACNA1B*, encoding the α1 subunit of NCCs, in either wild-type (WT) or dnNRSF-Tg hearts, which is in contrast to its obvious expression in brain (*Figure 1A*). On the other hand, we detected substantially greater ventricular expression of *CACNA1H*, encoding the α1 subunit of TCCs, and *CACNA1C*, encoding the α1 subunit of L-type Ca^{2+} channels (*Figure 1B*). Although ventricular expression of *CACNA1B* is increased in dnNRSF-Tg hearts, probably due to the presence of NRSF-binding element in the gene, the levels are still lower than those of *CACNA1H* in WT hearts, where no functional T-type Ca^{2+}currents are detected.[11,18] To evaluate the potential therapeutic effect of modulating autonomic nervous system activity through NCC blockade on the development of malignant arrhythmias and sudden death in dnNRSF-Tg mice, we administered subpressor doses of cilnidipine, a dual N- and L-type dihydropyridine Ca^{2+} channel blocker, or nitrendipine, a more L-type-selective dihydropyridine Ca^{2+} channel blocker, to dnNRSF-Tg mice for 24 weeks, beginning when they were 8 weeks of age. Under our experimental conditions, systolic blood pressures and heart rates did not differ among the control, cilnidipine, and nitrendipine groups

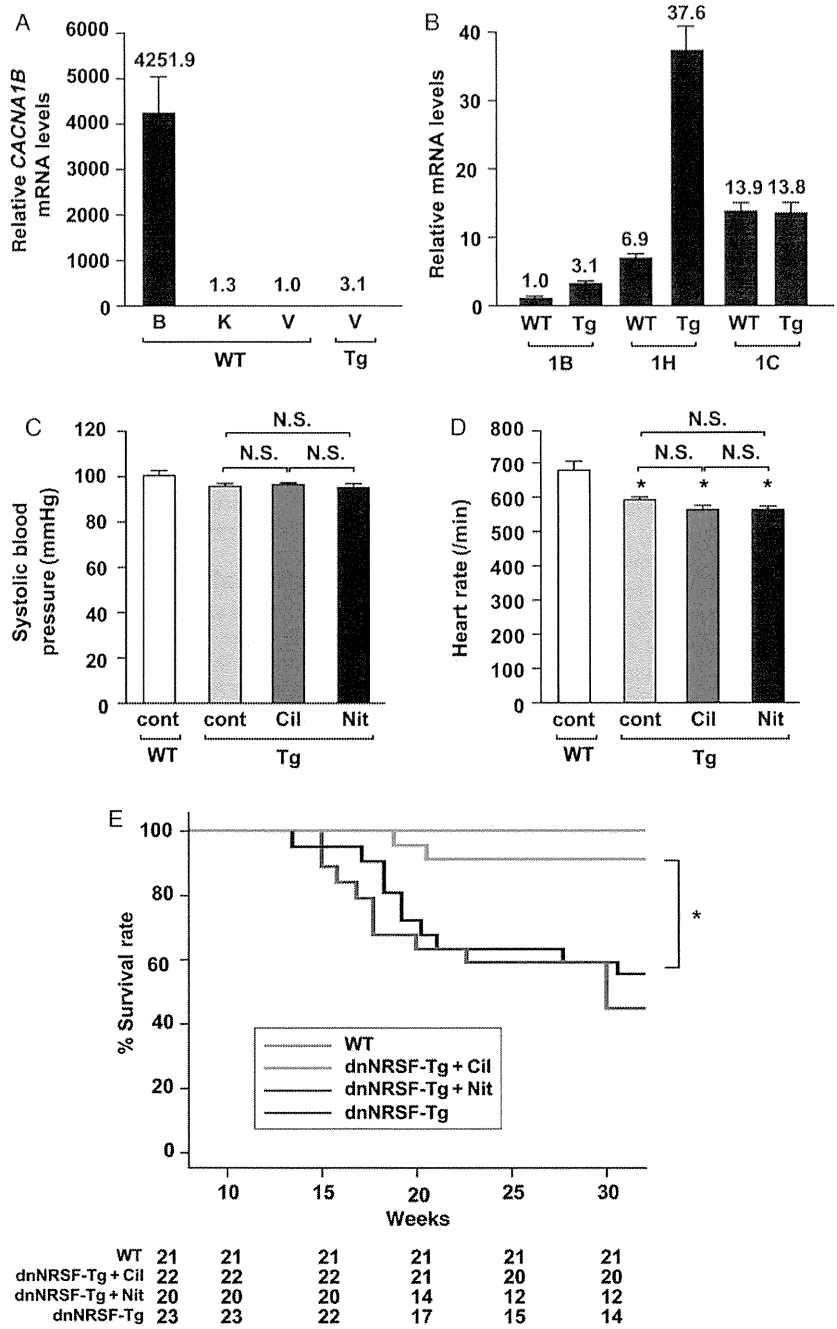

Figure 1 Pharmacological blockade of NCCs by cilnidipine improves survival among dnNRSF-Tg mice. (*A*) Relative levels of CACNA1B mRNA in brains (B) from WT, kidney (K) from WT, cardiac ventricle (V) from WT, and cardiac ventricle (V) from 8-week-old dnNRSF-Tg mice (Tg); levels in cardiac ventricle from WT mice were assigned a value of 1.0. $n = 3$ each for brain, kidney, and cardiac ventricle from WT mice and $n = 2$ for cardiac ventricle from dnNRSF-Tg mice. (*B*) Relative levels of CACNA1B, CACNA1H, and CACNA1C mRNA in cardiac ventricle from 8-week-old WT mice and dnNRSF-Tg mice (Tg); levels of CACNA1B mRNA in WT mice were assigned a value of 1.0. $n = 5$ for WT mice and $n = 7$ for dnNRSF-Tg. (*C* and *D*) Systolic blood pressures (*C*) and heart rates (*D*) in 20-week-old untreated WT, untreated Tg (Tg-cont), cilnidipine-treated Tg (Tg-Cil), and nitrendipine-treated Tg-Nit mice ($n = 15$ each for untreated Tg, Tg-Cil, and Tg-Nit, and $n = 10$ for untreated WT). ANOVA with post hoc Fisher's tests was used for analysis. $^*P < 0.05$. N.S.: not significant. (*E*) Kaplan–Meyer survival curves for untreated WT, untreated Tg, Cil-treated Tg, and Nit-treated Tg over a 24-week drug administration period (from 8 to 32 weeks of age): Log-rank test was used for analysis. $^*P < 0.05$ ($n = 21$ for WT, $n = 23$ for Tg without drugs, $n = 22$ for Tg + Cil, and $n = 20$ for Tg + Nit). The numbers of mice alive in each group at the end of each period are shown at the bottom of the figure. All data except survival curves are shown as means ± SEM.

of dnNRSF-Tg mice, though blood pressures were slightly lower and heart rates were significantly slower in dnNRSF-Tg mice than in untreated WT mice, as previously reported (systolic blood pressure: WT, 101.40 ± 1.48; Tg, 96.0 ± 1.75; Tg + cilnidipine, 96.67 ± 1.64; Tg + nitrendipine, 95.47 ± 1.92 mmHg and Heart rates: WT, 682.3 ± 27; dnNRSF-Tg, 590.6 ± 10.9; Tg + cilnidipine, 567.13 ± 17.58; Tg + nitrendipine, 568.8 ± 11.07/min) (*Figure 1C* and *D*).[8] We found that cilnidipine dramatically improved the survival rate among dnNRSF-Tg mice, compared with mice treated with nitrendipine or untreated control (*Figure 1E*). Although heart-to-body weight ratios were higher in dnNRSF-Tg than in WT mice, as reported previously,[8] heart-to-body weight ratios did not significantly differ among the control, cilnidipine, and nitrendipine groups of dnNRSF-Tg mice (WT, 4.08 ± 0.31; Tg, 5.94 ± 0.24; Tg + cilnidipine, 5.61 ± 0.48; Tg + nitrendipine, 5.94 ± 0.36 mg/g) (*Figure 2A*). Lung-to-body weight ratios also did not differ among these three groups (WT, 5.28 ± 0.37; Tg, 6.07 ± 0.22; Tg + cilnidipine, 5.93 ± 0.79; Tg + nitrendipine, 5.9 ± 0.29 mg/g) (*Figure 2B*). In addition, histological analyses, including determination of the %fibrotic area, and echocardiographic analyses also showed no significant differences among these three groups (*Figure 2C–F* and *Table 1*). In contrast, the echocardiography and histology showed that, compared with untreated WT mice, left ventricular systolic function was diminished and %fibrotic area was increased in dnNRSF-Tg mice, as reported previously (*Figure 2C–F* and *Table 1*).[8] Consistent with these findings, there was no significant difference in the expression of two cardiac stress marker genes, *ANP* and *SERCA2*, among the three groups, whereas their expression did differ between untreated WT mice and dnNRSF-Tg mice, as described previously (*Figure 2G* and *H*).[8]

Expression of the fibrosis-related genes *Col1a1*, *Col3a1*, and *FN1*, encoding collagen type1α1, collagen type3α1, and fibronectin 1, respectively, was not affected by the drug treatments (see Supplementary material online, *Figure S1A–C*). Expression of genes encoding the fetal-type ion channels *CACNA1H*, *HCN2*, and *HCN4* was higher in untreated dnNRSF-Tg ventricles than in control WT ventricles, as reported previously, and cilnidipine did not affect expression of these genes in dnNRSF-Tg ventricles (see Supplementary material online, *Figure S1D–F*). Collectively, all of these data indicate that cilnidipine suppresses sudden death in dnNRSF-Tg mice without significantly affecting cardiac structure or function.

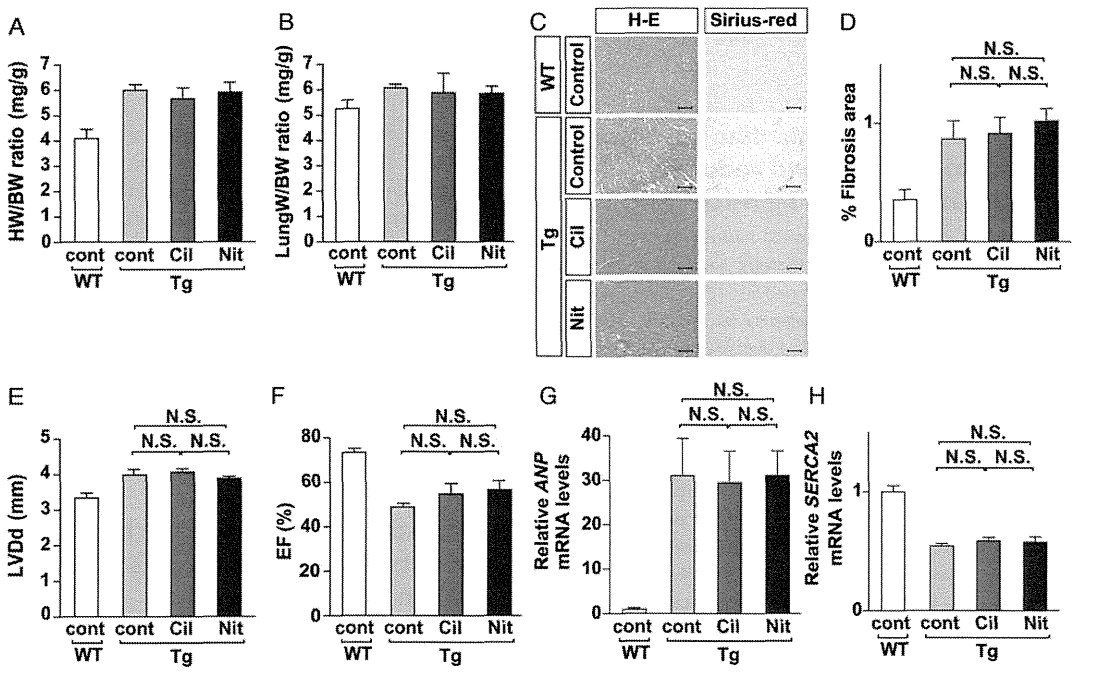

Figure 2 Cilnidipine does not affect cardiac structure or function in dnNRSF-Tg mice. (*A* and *B*) Heart-to-body weight (HW/BW) ratios (*A*) and lung-to-body weight (LungW/BW) ratios (*B*) in 20-week-old untreated WT (WT-cont), untreated Tg (Tg-cont), Cil-treated Tg (Tg-Cil), and Nit-treated Tg (Tg-Nit) mice ($n = 5$ for untreated WT, $n = 4$ for Tg-cont, $n = 4$ for Tg-Cil, and $n = 3$ for Tg-Nit). (*C*) Histology of hearts from 20-week-old untreated WT, Tg-cont, Tg-Cil, and Tg-Nit mice: H-E, haematoxylin-eosin staining; Sirius-red, Sirius-red staining. Scale bars = 100 μm. (*D*) %fibrotic area in 20-week-old untreated WT, Tg-cont, Tg-Cil, and Tg-Nit mice ($n = 5$ for Tg-cont; $n = 7$ for Tg-Cil). N.S.: not significant. (*E* and *F*) LVDd (*E*) and EF (*F*) assessed echocardiographically in untreated WT, Tg-cont, Tg-Cil, and Tg-Nit mice. *$P < 0.05$. N.S.: not significant. ($n = 5$ each for untreated WT, Tg-cont, and Tg-Cil; $n = 7$ for Tg-Nit). (*G* and *H*) Relative levels of ANP (*G*) and SERCA2 (*H*) mRNA in cardiac ventricles from untreated WT, Tg-cont, Tg-Cil, and Tg-Nit mice; levels in untreated WT were assigned a value of 1.0. N.S.: not significant. ($n = 4$ each). ANOVA with post hoc Fisher's tests was used for analysis. All data are shown as means ± SEM.

Table 1 Echocardiographic parameters in 20-week-old mice

	WT	dnNRSF-Tg		
	Control	Cont	Cil	Nit
Pharmacological inhibition				
LVDd (mm)	3.3 ± 0.13	3.9 ± 0.19	4.0 ± 0.11	3.8 ± 0.08
LVDs (mm)	2.1 ± 0.08	3.1 ± 0.17	3.1 ± 0.11	2.9 ± 0.10
IVST (mm)	0.76 ± 0.02	0.72 ± 0.02	0.72 ± 0.02	0.71 ± 0.03
PWT (mm)	0.76 ± 0.02	0.74 ± 0.02	0.76 ± 0.02	0.76 ± 0.03
FS (%)	36.1 ± 2.3	20.3 ± 1.4	23.3 ± 2.7	23.8 ± 2.4
EF (%)	73.2 ± 2.7	49.0 ± 2.3	55.4 ± 4.2	57.0 ± 4.3
			dnNRSF-Tg	
	$1B^{+/+}$	$1B^{+/-}$	$1B^{+/+}$	$1B^{+/-}$
Genetic titration				
LVDd (mm)	3.2 ± 0.10	3.3 ± 0.08	4.1 ± 0.12	3.3 ± 0.07*
LVDs (mm)	2.2 ± 0.12	2.2 ± 0.06	3.2 ± 0.13	2.3 ± 0.08*
IVST (mm)	0.66 ± 0.01	0.68 ± 0.02	0.66 ± 0.02	0.69 ± 0.02
PWT (mm)	0.68 ± 0.02	0.67 ± 0.02	0.66 ± 0.02	0.68 ± 0.02
FS (%)	31.8 ± 1.8	33.1 ± 1.9	20.4 ± 1.3	30.4 ± 1.3*
EF (%)	66.4 ± 2.4	68.9 ± 2.6	49.0 ± 2.4	64.3 ± 1.8*

Values are means ± SEM. Cil, cilnidipine; Nit, nitrendipine; $1B^{+/+}$, CACNA1B$^{+/+}$; $1B^{+/-}$, CACNA1B$^{+/-}$; LVDd, left ventricular diastolic dimension; LVDs, left ventricular systolic dimension; FS, fractional shortening; IVST, intraventricular septum wall thickness; PWT, posterior wall thickness. Numbers of mice tested in the pharmacological inhibition study are as follows: $n = 5$ for WT, untreated dnNRSF-Tg, and Cil-treated dnNRSF-Tg; $n = 7$ for Nit-treated dnNRSF-Tg (upper panel). Numbers of mice tested in the genetic titration study are as follows: $n = 13$ for $1B^{+/+}$, $n = 14$ for $1B^{+/-}$, $n = 11$ for dnNRSF-Tg;$1B^{+/+}$, and $n = 15$ for dnNRSF-Tg; $1B^{+/-}$ (lower panel). ANOVA with *post hoc* Fisher's tests was used for the analysis.
*$P < 0.05$ vs. dnNRSF-Tg;$1B^{+/+}$.

3.2 Cilnidipine improves cardiac autonomic nervous system function and reduces arrhythmicity in dnNRSF-Tg mice

We hypothesized that correcting autonomic balance through NCC blockade reduces arrhythmogenicity, thereby improving survival among dnNRSF-Tg mice. Heart rate variability (HRV) is a widely accepted index of cardiac autonomic nervous system activity.[19] Earlier frequency domain analysis of HRV revealed that patients with severe heart failure show a progressive reduction in power in both the low-frequency (LF) and high-frequency (HF) ranges,[19] and that a reduction in the LF power range is a significant predictor of sudden cardiac death in patients with heart failure.[20] We used HRV as an index to evaluate cardiac autonomic function in WT and dnNRSF-Tg mice, and examined the effects of cilnidipine on HRV.[19] In mice, HRV predominantly correlates with parasympathetic activity.[21] As we showed previously, both the LF and HF powers averaged over 24 h in dnNRSF-Tg mice (LF, 1.228 ± 0.198; HF, 0.823 ± 0.186 m/s^2) were markedly lower than in WT mice (LF, 4.331 ± 0.706; HF, 2.412 ± 0.089 m/s^2), indicating a general reduction in parasympathetic activity in dnNRSF-Tg mice (*Figure 3A* and *B*). Cilnidipine dramatically increased the power in both the LF and HF ranges of HRV (LF, 3.308 ± 0.338; HF, 2.228 ± 0.283 m/s^2), whereas nitrendipine had little effect on HRV (LF, 0.538 ± 0.447; HF, 1.383 ± 0.57 m/s^2) (*Figure 3A* and *B*). We also found that urinary excretion of norepinephrine, which is indicative of the level of sympathetic nerve activity, was significantly higher in dnNRSF-Tg than in WT mice, and that norepinephrine excretion was significantly reduced only by cilnidipine (WT, 0.09 ± 0.02; Tg, 0.33 ± 0.04; Tg + cilnidipine, 0.15 ± 0.03; Tg + nitrendipine, 0.32 ± 0.1 μg/day) (*Figure 3C*).

We next used an implanted telemetric monitoring system to examine the effects of cilnidipine and nitrendipine on electrocardiographic parameters in dnNRSF-Tg mice. We found that only cilnidipine significantly suppressed the number of premature ventricular contractions (PVCs) in dnNRSF-Tg hearts (WT, 0 ± 0; dnNRSF-Tg, 502.66 ± 305.69; dnNRSF-Tg + cilnidipine, 1.0 ± 0.66; dnNRSF-Tg + nitrendipine, 326.17 ± 147.24 /h) (*Figure 3D*). More importantly, it dramatically reduced the number of episodes of ventricular tachycardia (VT) (WT, 0 ± 0; dnNRSF-Tg, 14.92 ± 4.95; dnNRSF-Tg + cilnidipine, 0.06 ± 0.06; dnNRSF-Tg + nitrendipine, 12.75 ± 5.16/h) (*Figure 3E* and Supplementary material online, *Figure S2A* and *B*). These lines of evidence suggest that by restoring autonomic nervous system balance, cilnidipine reduces the incidence of lethal arrhythmias in dnNRSF-Tg mice.

3.3 β-Adrenergic receptor blockade prevents lethal arrhythmias and sudden death in dnNRSF-Tg mice

To verify the importance of correcting autonomic nervous system imbalance for the prevention of lethal arrhythmias and sudden death in dnNRSF-Tg mice, irrespective of effects on structural remodelling, we examined the effects of treating these mice with a β-adrenergic receptor blocker. We administered a subpressor dose of the lipophilic β-adrenergic receptor blocker bisoprolol (1 mg/kg/day po) to WT and dnNRSF-Tg mice. Although systolic blood pressures did not differ between untreated control and bisoprolol-treated mice (untreated WT, 107.5 ± 1.6; WT + bisoprolol, 108.0 ± 1.2; untreated Tg, 98.6 ± 2.0; Tg + bisoprolol, 98.6 ± 1.7 mmHg) (*Figure 3F*), heart rates were significantly slower in bisoprolol-treated than in untreated WT and dnNRSF-Tg mice (untreated WT, 697.8 ± 8.3; WT + bisoprolol,

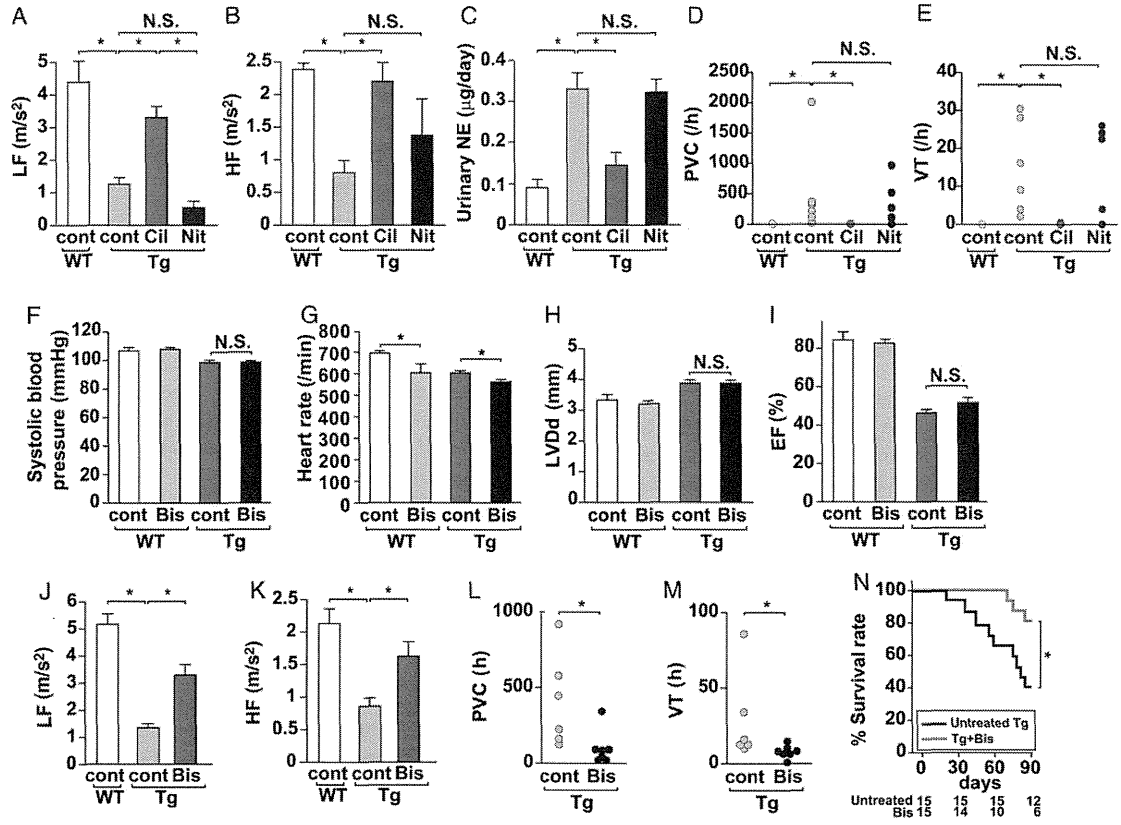

Figure 3 Cilnidipine restores cardiac autonomic nervous system balance and reduces arrhythmias in dnNRSF-Tg mice. (*A* and *B*) Average power of the LF (*A*) and HF (*B*) components of HRV recorded over a 24-h period in 20-week-old untreated WT (WT-cont), untreated Tg (Tg-cont), Cil-treated Tg (Tg-Cil), and Nit-treated (Tg-Nit) mice. $^*P < 0.05$. N.S.: not significant ($n = 5$ for WT, $n = 6$ for Tg-cont, $n = 8$ for Tg-Cil, and $n = 6$ for Tg-Nit). (*C*) Urinary norepinephrine (NE) levels in 20-week-old WT-cont, Tg-cont, Tg-Cil, and Tg-Nit mice. $^*P < 0.05$. N.S.: not significant ($n = 7$ for WT, $n = 7$ for Tg-cont, $n = 5$ for Tg-Cil, and $n = 4$ for Tg-Nit). (*D* and *E*) Numbers of PVC (*D*) and VT (*E*) recorded with a telemetry system in 20-week-old WT-cont, Tg-cont, Tg-Cil, and Tg-Nit mice are shown by dot plots. $^*P < 0.0083$, N.S.: not significant ($n = 5$ for WT-cont, $n = 6$ for Tg-cont, $n = 8$ for Tg-Cil, and $n = 6$ for Tg-Nit). (*F* and *G*) Systolic blood pressures (*F*) and heart rates (*G*) in 20-week-old untreated WT (WT-cont), bisoprolol (Bis)-treated WT (WT-Bis), untreated Tg (Tg-cont), and Bis-treated Tg (Tg-Bis) mice ($n = 4$ for WT-cont, $n = 3$ for WT-Bis, and $n = 5$ for Tg-cont and Tg-Bis). (*H* and *I*) LVDd (*H*) and EF (*I*) assessed echocardiographically in WT-cont, WT-Bis, Tg-cont, and Tg-Bis mice. $^*P < 0.05$. N.S.: not significant. ($n = 4$ for WT-cont, $n = 3$ for WT-Bis, and $n = 5$ for Tg-cont and Tg-Bis). (*J* and *K*) Average power of the LF (*J*) and HF (*K*) components of heart rate variability (HRV) recorded over a 24-h period in 20-week-old WT-cont, Tg-cont, and Tg-Bis mice. $^*P < 0.05$. N.S.: not significant ($n = 4$ for WT-cont, $n = 6$ for Tg-cont, and $n = 7$ for Tg-Bis). (*L* and *M*) Numbers of PVC (*L*) and VT (*M*) recorded with a telemetry system in 20-week-old Tg-cont and Tg-Bis mice are shown by dot plots. $^*P < 0.05$ ($n = 6$ for Tg-cont; $n = 7$ for Tg-Bis). ANOVA with post hoc Fisher's tests was used for analysis, except for numbers of arrhythmias (*D*, *E*, *L*, and *M*). Numbers of arrhythmias among the four groups were analyzed using Kruskal–Wallis non-parametric ANOVA followed by the Bonferroni correction (*D* and *E*). Numbers of arrhythmias between two groups were analyzed using non-parametric Mann–Whitney test (*L* and *M*). (*N*) Kaplan–Meyer survival curves for untreated Tg and Bis-treated Tg (Tg + Bis) over a 90-day drug administration period (from 12 to 25 weeks of age): Log-rank test was used for the survival analysis. $^*P < 0.05$ ($n = 15$ each). The numbers of mice alive in each group at the end of each period are shown at the bottom of the figure. All data except numbers of arrhythmias and survival curves are shown as means ± SEM.

604.7 ± 38.3; Tg, 601.6 ± 10.1; Tg + bisoprolol, 558.6 ± 12.0/min) (*Figure 3G*). At the dose tested, bisoprolol also did not affect cardiac systolic function assessed echocardiographically in dnNRSF-Tg mice [LVDd: WT, 3.3 ± 0.2; WT + bisoprolol, 3.2 ± 0.1; Tg, 3.9 ± 0.1; Tg + bisoprolol, 3.9 ± 0.1 mm and ejection fraction (EF): WT, 84.5 ± 4.0; WT + bisoprolol, 83.0 ± 1.5; Tg, 46.0 ± 1.6; Tg + bisoprolol, 51.5 ± 2.7%] (*Figure 3H* and *I*). On the other hand, bisoprolol significantly restored power in both the LF and HF ranges of HRV (LF: untreated WT, 5.19 ± 0.37; Tg, 1.36 ± 0.14; Tg + bisoprolol, 3.34 ± 0.39 m/s^2 and HF: untreated WT, 2.12 ± 0.24; Tg, 0.86 ± 0.12; Tg + bisoprolol, 1.62 ± 0.22 m/s^2) (*Figure 3J* and *K*) and reduced the incidence of PVCs and VTs in those mice (PVC: Tg, 408.3 ± 122.9; Tg + bisoprolol, 98.9 ± 42.2/h; VT: Tg, 28.2 ± 12.1; Tg + bisoprolol, 7.6 ± 1.7/h) (*Figure 3L* and *M*). As a result, bisoprolol significantly improved survival rates among dnNRSF-Tg mice (*Figure 3N*). These results strongly support our finding that imbalance of autonomic nervous system

activities is critically involved in the occurrence of sudden arrhythmic death in dnNRSF-Tg mice.

3.4 Genetic titration of NCC improves survival among dnNRSF-Tg mice

To further confirm the benefit of NCC inhibition for prevention of sudden death in dnNRSF-Tg mice, we next genetically titrated NCC expression by crossing dnNRSF-Tg mice with mice lacking *CACNA1B*, encoding the α1B subunit of NCC. Because the *CACNA1B*$^{-/-}$ genotype has a high incidence of early mortality from an as yet unknown cause, we compared the phenotypes of dnNRSF-Tg;*CACNA1B*$^{+/+}$ mice with those of dnNRSF-Tg;*CACNA1B*$^{+/-}$ mice, in which NCC expression is reduced to ~52.9% of that in dnNRSF-Tg;*CACNA1B*$^{+/+}$ mice (*Figure 4A*). The gross appearance of *CACNA1B*$^{+/-}$ mice is normal, and they show no early mortality. Systolic blood pressures in dnNRSF-Tg;*CACNA1B*$^{+/-}$ and dnNRSF-Tg;*CACNA1B*$^{+/+}$ mice did not significantly differ, but they were mildly lower than in control WT (*CACNA1B*$^{+/+}$) mice (WT, 101.25 ± 7.26; *CACNA1B*$^{+/-}$, 91.25 ± 2.78; dnNRSF-Tg, 92 ± 4.38; dnNRSF-Tg;*CACNA1B*$^{+/-}$, 89.25 ± 2.14 mmHg) (*Figure 4B*). Similarly, heart rates did not differ between dnNRSF-Tg;*CACNA1B*$^{+/+}$ and dnNRSF-Tg;*CACNA1B*$^{+/-}$ mice, although they were slower in dnNRSF-Tg;*CACNA1B*$^{+/+}$ than in control WT mice, as reported previously (WT, 632.25 ± 26.36; *CACNA1B*$^{+/-}$, 594 ± 33.39; dnNRSF-Tg, 515.25 ± 14.71; dnNRSF-Tg;*CACNA1B*$^{+/-}$, 521.5 ± 23.32/min) (*Figure 4C*).[8] Body weights were comparable between the two dnNRSF-Tg groups (WT, 31.08 ± 1.11; *CACNA1B*$^{+/-}$, 29.53 ± 1.37; dnNRSF-Tg; 28.86 ± 1.19; dnNRSF-Tg;*CACNA1B*$^{+/-}$, 27.41 ± 1.09 g) (*Figure 4D*), but heart-to-body weight ratios were higher in dnNRSF-Tg;*CACNA1B*$^{+/+}$ than in WT (*CACNA1B*$^{+/+}$) mice and were significantly lower in dnNRSF-Tg;*CACNA1B*$^{+/-}$ than in dnNRSF-Tg;*CACNA1B*$^{+/+}$ mice (WT, 4.44 ± 0.04; *CACNA1B*$^{+/-}$, 4.51 ± 0.14; dnNRSF-Tg; 5.68 ± 0.21; dnNRSF-Tg;*CACNA1B*$^{+/-}$, 4.86 ± 0.18 mg/g) (*Figure 4E*). Lung-to-body weight ratios were comparable between the two dnNRSF-Tg groups (WT, 5.06 ± 0.22; *CACNA1B*$^{+/-}$, 4.68 ± 0.96; dnNRSF-Tg; 5.41 ± 0.09; dnNRSF-Tg; *CACNA1B*$^{+/-}$, 5.52 ± 0.26 mg/g) (*Figure 4F*). Echocardiographic analysis showed that left ventricular diastolic dimension (LVDd) was higher in dnNRSF-Tg;*CACNA1B*$^{+/+}$ than in WT mice, whereas EF was lower in dnNRSF-Tg;*CACNA1B*$^{+/+}$ than in WT mice, as was reported previously (*Figure 5A* and *B*).[8] In addition, LVDd was lower and EF was higher in dnNRSF-Tg;*CACNA1B*$^{+/-}$ than in dnNRSF-Tg;*CACNA1B*$^{+/+}$ mice (*Figure 5A* and *B* and *Table 1*).

Histological analysis revealed no significant difference between dnNRSF-Tg;*CACNA1B*$^{+/+}$ and dnNRSF-Tg;*CACNA1B*$^{+/-}$ mice, although %fibrotic area showed a trend towards being smaller in dnNRSF-Tg;*CACNA1B*$^{+/-}$ than in dnNRSF-Tg;*CACNA1B*$^{+/+}$ mice (*Figure 5C* and *D*). Expression of the fibrosis-related genes *Col1a1*, *Col3a1*, and *FN1* did not significantly differ between dnNRSF-Tg;*CACNA1B*$^{+/+}$ and dnNRSF-Tg;*CACNA1B*$^{+/-}$ mice (see Supplementary material online, *Figure S3A–C*), though there was a significant difference in the expression of *ANP* and *SERCA2* between these two genotypes (*Figure 5E* and *F*). Genetic reduction in *CACNA1B* also significantly affected expression of *CACNA1H* and *HCN2*, but not *HCN4*, in dnNRSF-Tg ventricles (see Supplementary material online, *Figure S3D–F*). All of these data demonstrate that genetic reduction of *CACNA1B* tends to ameliorate impaired cardiac function and pathological remodelling in dnNRSF-Tg mice. Furthermore, survival among dnNRSF-Tg;*CACNA1B*$^{+/-}$ mice was dramatically and significantly better than among control dnNRSF-Tg;*CACNA1B*$^{+/+}$ mice (*Figure 6A*), demonstrating that reduction of NCC prevents sudden arrhythmic death in dnNRSF-Tg mice.

3.5 Reducing *CACNA1B* expression improves autonomic function and decreases the occurrence of arrhythmias in dnNRSF-Tg mice

We also assessed autonomic nervous system activity in dnNRSF-Tg;*CACNA1B*$^{+/-}$ and dnNRSF-Tg;*CACNA1B*$^{+/+}$ mice. In HRV analyses, the reductions in LF and HF power otherwise seen in dnNRSF-Tg;*CACNA1B*$^{+/+}$ mice (LF, 1.288 ± 0.16; HF, 1.168 ± 0.108 m/s^2) were significantly ameliorated in dnNRSF-Tg;*CACNA1B*$^{+/-}$ mice (LF, 3.54 ± 0.47; HF, 3.075 ± 0.468 m/s^2), indicating a restoration of parasympathetic activity through reduction of NCC function (*Figure 6B* and *C*). In addition, we found that the increase in urinary excretion of norepinephrine seen in dnNRSF-Tg;*CACNA1B*$^{+/+}$ mice (0.428 ± 0.07 μg/day) was significantly ameliorated in dnNRSF-Tg;*CACNA1B*$^{+/-}$ mice (0.154 ± 0.05 μg/day) (*Figure 6D*). Finally, evaluation of arrhythmicity revealed that the incidences of both PVCs and VT were significantly lower in dnNRSF-Tg;*CACNA1B*$^{+/-}$ than in dnNRSF-Tg;*CACNA1B*$^{+/+}$ mice (PVC: WT, 0 ± 0; *CACNA1B*$^{+/-}$, 0 ± 0; dnNRSF-Tg, 239.08 ± 27.93; dnNRSF-Tg;*CACNA1B*$^{+/-}$, 3.21 ± 3.21 and VT: WT, 0 ± 0; *CACNA1B*$^{+/-}$, 0 ± 0; dnNRSF-Tg, 41.3 ± 12.69; dnNRSF-Tg;*CACNA1B*$^{+/-}$, 0.36 ± 0.36/h) (*Figure 6E* and *F*). These results demonstrate that genetic titration of *CACNA1B*, encoding NCC, corrected an imbalance between sympathetic and parasympathetic nervous system activities, which, at least in part, contributes to reducing malignant arrhythmias in dnNRSF-Tg mice in a manner similar to pharmacological NCC blockade.

4. Discussion

Autonomic dysregulation leading to increased sympathetic nerve activity and reduced parasympathetic nerve activity is reportedly associated with the increased arrhythmicity seen in patients with chronic heart failure.[2,22,23] NCCs play a major role in the release of norepinephrine at sympathetic nerve terminals.[7,24] Consequently, mice lacking *CACNA1B*, the gene encoding the α1 subunit of NCCs, exhibit a significantly impaired positive inotropic response.[7] In the present study, we found that pharmacological blockade of NCCs or their genetic titration improved the balance between sympathetic and parasympathetic nerve activities and prevented the sudden death and arrhythmicity otherwise seen in dnNRSF-Tg mice, a mouse model of sudden arrhythmic death associated with cardiac dysfunction.[8] The mode of death in these model mice is sudden and without overt oedema, pleural effusion, or apparent lung congestion, and all the telemetry data obtained at the time of death indicate VT/VF to be the cause.[8] Moreover, in an earlier study, we found that systemic administration of isoproterenol induced VT more frequently in dnNRSF-Tg than in WT mice.[11] Conversely, administration of a β-blocker led to a significant reduction in the incidence of sudden death among dnNRSF-Tg mice under conditions in which cardiac systolic function and remodelling were not affected (*Figure 3H–N*). These findings suggest that NCC blockade or genetic titration of NCC reduces the likelihood of sudden arrhythmic death, thereby improving survival.

Pharmacological interventions that reduce cardiac sympathetic activity have been shown to protect against arrhythmias,[25] while

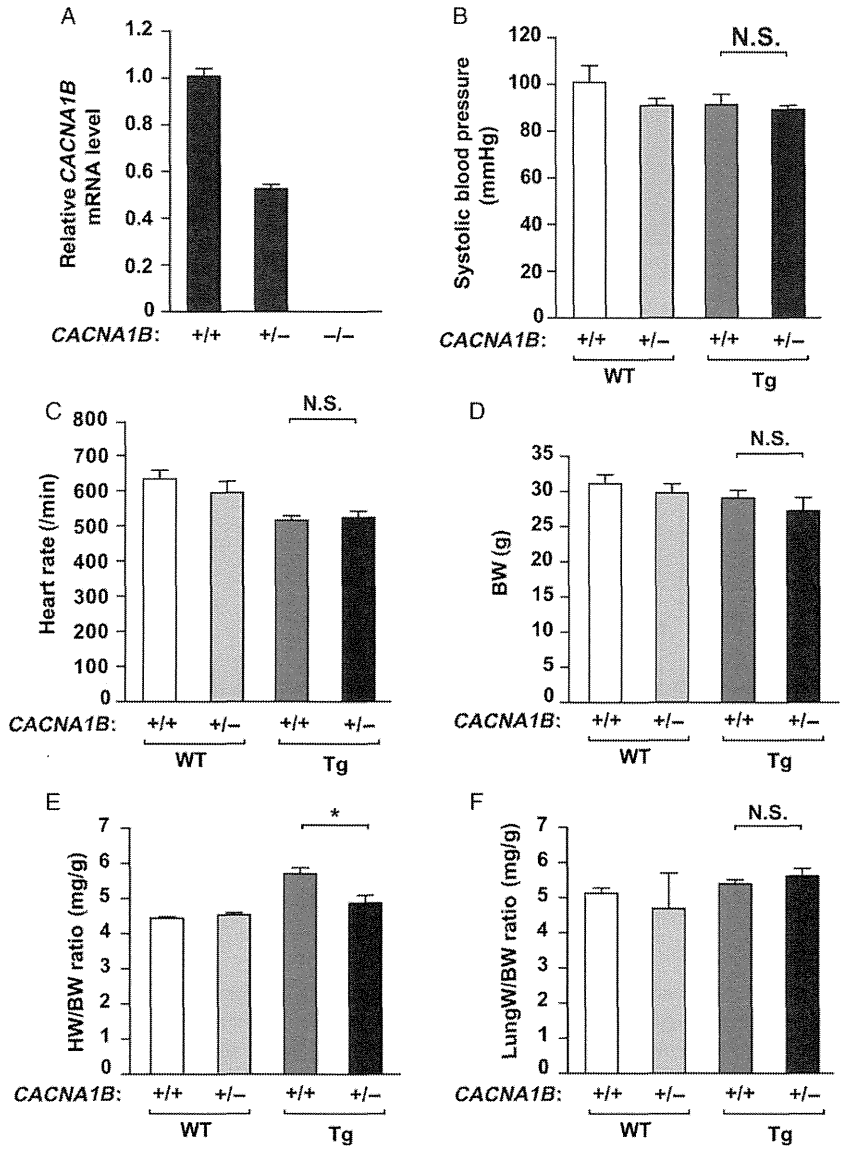

Figure 4 Effects of genetic titration of *CACNA1B* on hemodynamics and heart size in WT and dnNRSF-Tg mice. (*A*) CACNA1B mRNA expression in brains from 8-week-old CACNA1B$^{+/+}$, CACNA1B$^{+/-}$, and CACNA1B$^{-/-}$ mice; the level in CACNA1B$^{+/+}$ brain was assigned a value of 1.0. (*B* and *C*) Systolic blood pressures (*B*) and heart rates (*C*) in 20-week-old CACNA1B$^{+/+}$, CACNA1B$^{+/-}$, dnNRSF-Tg;CACNA1B$^{+/+}$, and dnNRSF-Tg;CACNA1B$^{+/-}$ mice. N.S.: not significant ($n = 4$ each). (*D*, *E*, and *F*) body weights (BW)(*D*), heart-to-body weight ratios (HW/BW) (*E*), and lung-to-body weight ratios (LungW/BW) (*F*) in 20-week-old CACNA1B$^{+/+}$, CACNA1B$^{+/-}$, dnNRSF-Tg;CACNA1B$^{+/+}$, and dnNRSF-Tg;CACNA1B$^{+/-}$ mice. *$P < 0.05$. N.S.: not significant. (BW and HW/BW: $n = 4$ for CACNA1B$^{+/+}$, $n = 6$ for CACNA1B$^{+/-}$, $n = 5$ for dnNRSF-Tg;CACNA1B$^{+/+}$, and $n = 7$ for dnNRSF-Tg;CACNA1B$^{+/-}$; LungW/BW: $n = 4$ for CACNA1B$^{+/+}$, $n = 6$ for CACNA1B$^{+/-}$ and dnNRSF-Tg;CACNA1B$^{+/-}$, and $n = 5$ for dnNRSF-Tg;CACNA1B$^{+/+}$). ANOVA with post hoc Fisher's tests was used for analysis. All data are shown as means ± SEM.

interventions that stimulate cardiac sympathetic activity provoke malignant arrhythmias.[2,26] In patients with heart failure, β-adrenoreceptor blockade reduces the incidence of sudden death;[27,28] however, β-blockers are not completely protective, and mortality remains high among patients with cardiac dysfunction, despite optimal β-blocker therapy.[27,28] It is therefore necessary to find other approaches to modulate sympathetic or parasympathetic activity. In that context, a clinical trial testing the effect of central modulation of sympathetic activity using moxonidine SR in patients with heart failure was terminated early due to an increase in mortality and morbidity in patients receiving the drug.[29] Thus, strong central inhibition of the sympathetic nervous system through imidazoline receptor stimulation appears not to

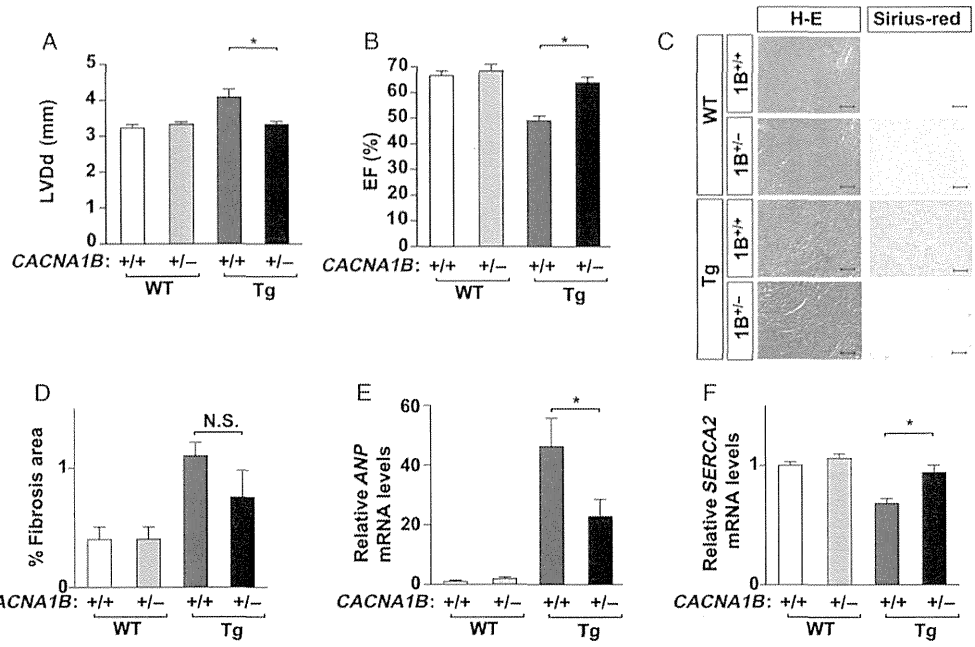

Figure 5 Effect of genetic titration of *CACNA1B* on cardiac structure and function in dnNRSF-Tg mice. (*A* and *B*) LVDd and EF assessed echocardiographically in 20-week-old CACNA1B$^{+/+}$, CACNA1B$^{+/-}$, CACNA1B$^{+/+}$; dnNRSF-Tg and CACNA1B$^{+/-}$; dnNRSF-Tg mice. *$P < 0.05$. ($n = 13$ for CACNA1B$^{+/+}$, $n = 14$ for CACNA1B$^{+/-}$, $n = 11$ for dnNRSF-Tg;CACNA1B$^{+/+}$, and $n = 15$ for dnNRSF-Tg;CACNA1B$^{+/-}$). (*C*) Histology of hearts from 20-week-old CACNA1B$^{+/+}$, CACNA1B$^{+/-}$, dnNRSF-Tg;CACNA1B$^{+/+}$ and dnNRSF-Tg;CACNA1B$^{+/-}$ mice. H-E, haematoxylin-eosin staining; Sirius-red, Sirius-red staining. Scale bars = 100 μm. (*D*) %Fibrotic area in the indicated groups ($n = 4$ for CACNA1B$^{+/+}$, $n = 6$ for CACNA1B$^{+/-}$, $n = 5$ for dnNRSF-Tg;CACNA1B$^{+/+}$, and $n = 7$ for dnNRSF-Tg;CACNA1B$^{+/-}$). N.S.: not significant. (*E* and *F*) Relative levels of ANP and SERCA2 mRNA in cardiac ventricles from 20-week-old CACNA1B$^{+/+}$, CACNA1B$^{+/-}$, dnNRSF-Tg;CACNA1B$^{+/+}$ and dnNRSF-Tg;CACNA1B$^{+/-}$ mice ($n = 4$ for CACNA1B$^{+/+}$, $n = 6$ for CACNA1B$^{+/-}$, and $n = 5$ for dnNRSF-Tg;CACNA1B$^{+/+}$ and dnNRSF-Tg;CACNA1B$^{+/-}$); levels in CACNA1B$^{+/+}$ ventricles were assigned a value of 1.0. *$P < 0.05$. ANOVA with post hoc Fisher's tests was used for analysis. All data are shown as means ± SEM.

protect against lethal arrhythmias. NCCs are localized at peripheral sympathetic nerve terminals, where they regulate the release of neurotransmitters (e.g. catecholamines), thereby modulating sympathetic activity.[4–6] Our findings suggest that, by correcting their autonomic dysregulation, NCC blockade could be an effective approach to preventing sudden arrhythmic death in patients with heart failure.

Cilnidipine failed to prevent the decline in cardiac function in dnNRSF-Tg mice, whereas genetic titration tended to ameliorate the adverse cardiac remodelling and cardiac dysfunction seen in dnNRSF-Tg mice (*Figures 2A–H*, *4E*, and *5A–F* and *Table 1*). The reasons for the difference in the effects on cardiac function between cilnidipine and genetic titration of NCCs remain unclear at present. It may be that cilnidipine's ability to block L-type Ca^{2+} channels has a detrimental effect on cardiac function, as L-type Ca^{2+} channel blockers can adversely affect the progression of heart failure.[30] Other possibilities are that the relatively low dose of cilnidipine used in this study was not sufficient to prevent the progression of cardiac dysfunction, though it did prevent lethal arrhythmias, or that the NCC inhibition achieved in *CACNA1B*$^{+/-}$ mice was more prolonged and more stable than that achieved with cilnidipine, which was not started until the mice were 8 weeks of age. The effects on NCCs expressed in the central nervous system could also differ between cilnidipine and genetic titration, as cilnidipine has little ability to cross the blood–brain barrier.[31] These differences suggest the underlying mechanisms involved in the reduced incidence of lethal arrhythmias, and the prolonged survival differ somewhat between cilnidipine treatment and genetic titration of *CACNA1B* in this study. Cilnidipine treatment, which improved autonomic imbalance and reduced lethal arrhythmias without affecting cardiac remodelling, mainly suppressed the triggering of lethal arrhythmias induced by autonomic imbalance. On the other hand, genetic titration of *CACNA1B*, which improved autonomic imbalance and also tended to prevent adverse cardiac remodelling, suppressed lethal arrhythmias and improved survival in two ways: it inhibited the triggering of arrhythmias and also suppressed the generation of arrhythmogenic substrates. In both cases, correcting the autonomic imbalance associates with a reduction in the incidence of sudden death attributable to lethal arrhythmias in dnNRSF-Tg. However, because it is not possible to completely exclude the possibility that some dnNRSF-Tg mice (especially older mice) die due to congestive heart failure, irrespective of arrhythmias, there is a possibility that genetic deletion of NCC may also prevent this mode of death in addition to sudden arrhythmic death in dnNRSF-Tg mice through suppression of excessive sympathetic activity.

In the present study, both pharmacological blockade of NCCs and their genetic titration not only repressed sympathetic activity, as demonstrated by a reduction in urinary norepinephrine levels, but also restored parasympathetic activity, as indicated by HRV analyses. The precise

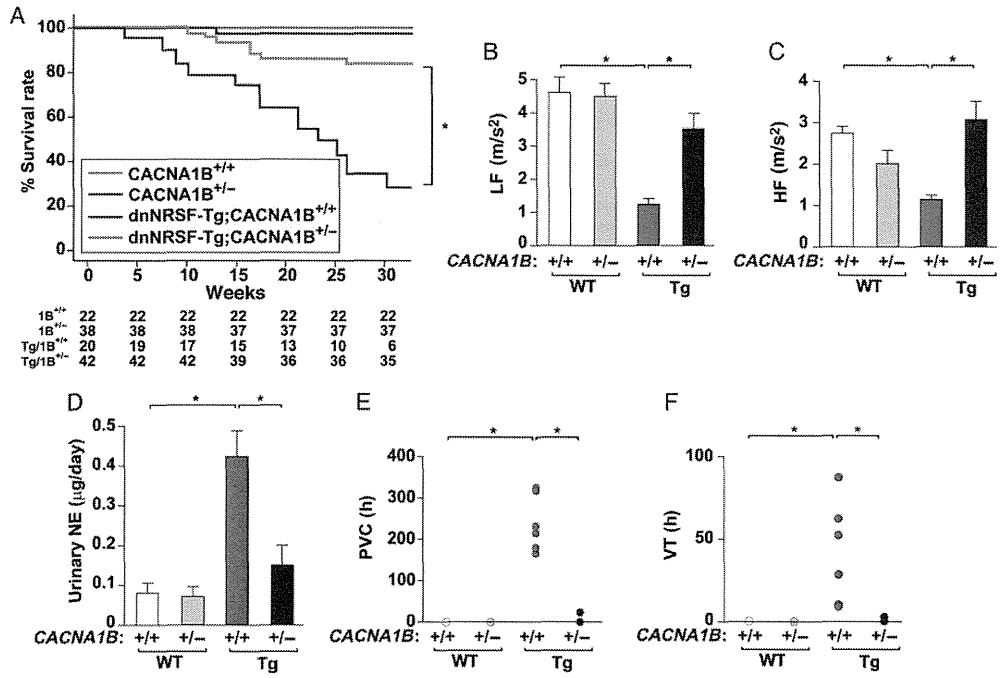

Figure 6 Genetic titration of *CACNA1B* restores cardiac autonomic nervous system balance and reduces arrhythmias in dnNRSF-Tg mice. (*A*) Kaplan–Meyer survival curves for CACNA1B$^{+/+}$ (1B$^{+/+}$), CACNA1B$^{+/-}$ (1B$^{+/-}$), dnNRSF-Tg;CACNA1B$^{+/+}$ (Tg/1B$^{+/+}$), and dnNRSF-Tg;CACNA1B$^{+/-}$ (Tg/1B$^{+/-}$) mice. Curves cover the span from birth to 32 weeks of age. Log-rank test was used for analysis. *$P < 0.05$ ($n = 22$ for CACNA1B$^{+/+}$, $n = 38$ for CACNA1B$^{+/-}$, $n = 20$ for dnNRSF-Tg;CACNA1B$^{+/+}$, and $n = 42$ for dnNRSF-Tg;CACNA1B$^{+/-}$). The numbers of mice alive in each group at the end of each period are shown at the bottom of the figure. (*B* and *C*) Average power of the LF (*B*) and HF (*C*) components of heart rate variability (HRV) recorded over a 24-h period in 20-week-old CACNA1B$^{+/+}$, CACNA1B$^{+/-}$, dnNRSF-Tg;CACNA1B$^{+/+}$, and dnNRSF-Tg;CACNA1B$^{+/-}$ mice. *$P < 0.05$ ($n = 5$ for CACNA1B$^{+/+}$, $n = 7$ for CACNA1B$^{+/-}$, $n = 6$ for dnNRSF-Tg;CACNA1B$^{+/+}$, and $n = 7$ for dnNRSF-Tg;CACNA1B$^{+/-}$). (*D*) Urinary norepinephrine (NE) levels in 20-week-old CACNA1B$^{+/+}$, CACNA1B$^{+/-}$, dnNRSF-Tg;CACNA1B$^{+/+}$, and dnNRSF-Tg;CACNA1B$^{+/-}$ mice. *$P < 0.05$ ($n = 5$ for CACNA1B$^{+/-}$, $n = 6$ for CACNA1B$^{+/+}$, dnNRSF-Tg;CACNA1B$^{+/+}$, and dnNRSF-Tg;CACNA1B$^{+/-}$). (*E* and *F*) Numbers of PVC (*E*) and VT (*F*) recorded using a telemetry system in 20-week-old CACNA1B$^{+/+}$, CACNA1B$^{+/-}$, dnNRSF-Tg;CACNA1B$^{+/+}$, and dnNRSF-Tg;CACNA1B$^{+/-}$ mice are shown by dot plot. *$P < 0.0083$ ($n = 5$ for CACNA1B$^{+/+}$, $n = 7$ for CACNA1B$^{+/-}$, $n = 6$ for dnNRSF-Tg;CACNA1B$^{+/+}$, and $n = 7$ for dnNRSF-Tg;CACNA1B$^{+/-}$). All data in *B*–*D* are shown as means ± SEM. ANOVA with post hoc Fisher's tests was used for analysis, except for numbers of arrhythmias (*E* and *F*). Numbers of arrhythmias were analyzed using Kruskal–Wallis non-parametric ANOVA followed by the Bonferroni correction.

mechanism by which NCC inhibition improves parasympathetic activity is not clear at present. However, accumulating data indicate the sympathetic and parasympathetic nervous systems interact via several mechanisms at both the central and peripheral levels of the neuraxis.[32] NCC inhibition-induced reductions in sympathetic activity may affect these interactions, ameliorating the reduction in parasympathetic activity, as was observed in dnNRSF-Tg mice. In humans, cilnidipine reportedly enhances parasympathetic activity in hypertensive patients while exerting a concomitant sympathoinhibitory effect.[12,13] Moreover, there is now much evidence showing the anti-arrhythmic effects of parasympathetic nervous activation. This suggests that, in addition to a reduction in sympathetic activity, an increase in parasympathetic activity likely contributes to the protective effects of NCC inhibition observed in this study.[27] Although further investigation is necessary, our study suggests that agents able to selectively block NCCs could be clinically useful for the prevention of sudden arrhythmic death in patients with heart failure.

Supplementary material

Supplementary material is available at *Cardiovascular Research* online.

Acknowledgements

We thank Ms Yukari Kubo for her excellent secretarial work and Ms Aoi Fujishima, Ms Akiko Abe, Mr Miku Ohya, and Ms Mizuho Takemura for their excellent technical support.

Conflict of interest: none declared.

Funding

This research was supported by Grants-in-Aid for Scientific Research from the Japan Society for the Promotion of Science (23390210, 24659386 to K.K., 24591095 to H.K., 22590810 to Y.N., 21229013 to N.K.); the Japanese Ministry of Health, Labor and Welfare (N.K.); the Japan Foundation for Applied Enzymology (K.K.); the UBE foundation (K.K.); the Ichiro Kanehara

Foundation (K.K.); the Takeda Science Foundation (K.K.); the Hoh-ansha Foundation (K.K.); the SENSHIN Medical Research Foundation (K.K.).

References

1. Tomaselli GF, Marban E. Electrophysiological remodeling in hypertrophy and heart failure. *Cardiovasc Res* 1999;**42**:270–283.
2. Anderson KP. Sympathetic nervous system activity and ventricular tachyarrhythmias: recent advances. *Ann Noninvasive Electrocardiol* 2003;**8**:75–89.
3. Chen PS, Chen LS, Cao JM, Sharifi B, Karagueuzian HS, Fishbein MC. Sympathetic nerve sprouting, electrical remodeling and the mechanisms of sudden cardiac death. *Cardiovasc Res* 2001;**50**:409–416.
4. Mori Y, Nishida M, Shimizu S, Ishii M, Yoshinaga T, Ino M, Sawada K, Niidome T. Ca(2+) channel alpha(1B) subunit (Ca(V) 2.2) knockout mouse reveals a predominant role of N-type channels in the sympathetic regulation of the circulatory system. *Trends Cardiovasc Med* 2002;**12**:270–275.
5. Hirning LD, Fox AP, McCleskey EW, Olivera BM, Thayer SA, Miller RJ, Tsien RW. Dominant role of N-type Ca2+ channels in evoked release of norepinephrine from sympathetic neurons. *Science* 1988;**239**:57–61.
6. Fujita Y, Mynlieff M, Dirksen RT, Kim MS, Niidome T, Nakai J, Friedrich T, Iwabe N, Miyata T, Furuichi T, Furutama D, Mikoshiba K, Mori Y, Beam KG. Primary structure and functional expression of the omega-conotoxin-sensitive N-type calcium channel from rabbit brain. *Neuron* 1993;**10**:585–598.
7. Ino M, Yoshinaga T, Wakamori M, Miyamoto N, Takahashi E, Sonoda J, Kagaya T, Oki T, Nagasu T, Nishizawa Y, Tanaka I, Imoto K, Aizawa S, Koch S, Schwartz A, Niidome T, Sawada K, Mori Y. Functional disorders of the sympathetic nervous system in mice lacking the alpha 1B subunit (Cav 2.2) of N-type calcium channels. *Proc Natl Acad Sci USA* 2001;**98**:5323–5328.
8. Kuwahara K, Saito Y, Takano M, Arai Y, Yasuno S, Nakagawa Y, Takahashi N, Adachi Y, Takemura G, Horie M, Miyamoto Y, Morisaki T, Kuratomi S, Noma A, Fujiwara H, Yoshimasa Y, Kinoshita H, Kawakami R, Kishimoto I, Nakanishi M, Usami S, Harada M, Nakao K. NRSF regulates the fetal cardiac gene program and maintains normal cardiac structure and function. *EMBO J* 2003;**22**:6310–6321.
9. Kuwabara Y, Kuwahara K, Takano M, Kinoshita H, Arai Y, Yasuno S, Nakagawa Y, Igata S, Usami S, Minami T, Yamada Y, Nakao K, Yamada C, Shibata J, Nishikimi T, Ueshima K, Nakao K. Increased expression of HCN channels in the ventricular myocardium contributes to enhanced arrhythmicity in mouse failing hearts. *J Am Heart Assoc* 2013;**2**: e000150.
10. Takano M, Kinoshita H, Shioya T, Itoh M, Nakao K, Kuwahara K. Pathophysiological remodeling of mouse cardiac myocytes expressing dominant negative mutant of neuron restrictive silencing factor. *Circ J* 2010;**74**:2712–2719.
11. Kinoshita H, Kuwahara K, Takano M, Arai Y, Kuwabara Y, Yasuno S, Nakagawa Y, Nakanishi M, Harada M, Fujiwara M, Murakami M, Ueshima K, Nakao K. T-type Ca2+ channel blockade prevents sudden death in mice with heart failure. *Circulation* 2009; **120**:743–752.
12. Kishi T, Hirooka Y, Konno S, Sunagawa K. Cilnidipine inhibits the sympathetic nerve activity and improves baroreflex sensitivity in patients with hypertension. *Clin Exp Hypertens* 2009;**31**:241–249.
13. Ogura C, Ono K, Miyamoto S, Ikai A, Mitani S, Sugimoto N, Tanaka S, Fujita M. L/T-type and L/N-type calcium-channel blockers attenuate cardiac sympathetic nerve activity in patients with hypertension. *Blood Press* 2012;**21**:367–371.
14. Egashira N, Okuno R, Abe M, Matsushita M, Mishima K, Iwasaki K, Oishi R, Nishimura R, Matsumoto Y, Fujiwara M. Calcium-channel antagonists inhibit marble-burying behavior in mice. *J Pharmacol Sci* 2008;**108**:140–143.
15. Lei B, Nakano D, Fujisawa Y, Liu Y, Hitomi H, Kobori H, Mori H, Masaki T, Asanuma K, Tomino Y, Nishiyama A. N-type calcium channel inhibition with cilnidipine elicits glomerular podocyte protection independent of sympathetic nerve inhibition. *J Pharmacol Sci* 2012;**119**:359–367.
16. Uneyama H, Uchida H, Konda T, Yoshimoto R, Akaike N. Selectivity of dihydropyridines for cardiac L-type and sympathetic N-type Ca2+ channels. *Eur J Pharmacol* 1999;**373**: 93–100.
17. Fujii S, Kameyama K, Hosono M, Hayashi Y, Kitamura K. Effect of cilnidipine, a novel dihydropyridine Ca++-channel antagonist, on N-type Ca++ channel in rat dorsal root ganglion neurons. *J Pharmacol Exp Ther* 1997;**280**:1184–1191.
18. Johnson R, Gamblin RJ, Ooi L, Bruce AW, Donaldson IJ, Westhead DR, Wood IC, Jackson RM, Buckley NJ. Identification of the REST regulon reveals extensive transposable element-mediated binding site duplication. *Nucleic Acids Res* 2006;**34**:3862–3877.
19. Heart rate variability. Standards of measurement, physiological interpretation, and clinical use. Task Force of the European Society of Cardiology and the North American Society of Pacing and Electrophysiology. *Eur Heart J* 1996;**17**:354–381.
20. La Rovere MT, Pinna GD, Maestri R, Mortara A, Capomolla S, Febo O, Ferrari R, Franchini M, Gnemmi M, Opasich C, Riccardi PG, Traversi E, Cobelli F. Short-term heart rate variability strongly predicts sudden cardiac death in chronic heart failure patients. *Circulation* 2003;**107**:565–570.
21. Just A, Faulhaber J, Ehmke H. Autonomic cardiovascular control in conscious mice. *Am J Physiol Regul Integr Comp Physiol* 2000;**279**:R2214–e002221.
22. Brack KE, Winter J, Ng GA. Mechanisms underlying the autonomic modulation of ventricular fibrillation initiation-tentative prophylactic properties of vagus nerve stimulation on malignant arrhythmias in heart failure. *Heart Fail Rev* 2013;**18**:389–408.
23. Schwartz PJ, La Rovere MT, Vanoli E. Autonomic nervous system and sudden cardiac death. Experimental basis and clinical observations for post-myocardial infarction risk stratification. *Circulation* 1992;**85**:I77–I91.
24. Molderings GJ, Likungu J, Gothert M. N-Type calcium channels control sympathetic neurotransmission in human heart atrium. *Circulation* 2000;**101**:403–407.
25. Billman GE. Cardiac autonomic neural remodeling and susceptibility to sudden cardiac death: effect of endurance exercise training. *Am J Physiol Heart Circ Physiol* 2009;**297**: H1171–H1193.
26. Volders PG. Novel insights into the role of the sympathetic nervous system in cardiac arrhythmogenesis. *Heart Rhythm* 2010;**7**:1900–1906.
27. Packer M, Coats AJ, Fowler MB, Katus HA, Krum H, Mohacsi P, Rouleau JL, Tendera M, Castaigne A, Roecker EB, Schultz MK, DeMets DL. Effect of carvedilol on survival in severe chronic heart failure. *N Engl J Med* 2001;**344**:1651–1658.
28. The Cardiac Insufficiency Bisoprolol Study II (CIBIS-II): a randomised trial. *Lancet* 1999; **353**:9–13.
29. Cohn JN, Pfeffer MA, Rouleau J, Sharpe N, Swedberg K, Straub M, Wiltse C, Wright TJ. Adverse mortality effect of central sympathetic inhibition with sustained-release moxonidine in patients with heart failure (MOXCON). *Eur J Heart Fail* 2003;**5**:659–667.
30. Mahe I, Chassany O, Grenard AS, Caulin C, Bergmann JF. Defining the role of calcium channel antagonists in heart failure due to systolic dysfunction. *Am J Cardiovasc Drugs* 2003;**3**:33–41.
31. Watanabe K, Dozen M, Hayashi Y. Effect of cilnidipine (FRC-8653) on autoregulation of cerebral blood flow. *Nihon Yakurigaku Zasshi* 1995;**106**:393–399.
32. Ondicova K, Mravec B. Multilevel interactions between the sympathetic and parasympathetic nervous systems: a minireview. *Endocr Regul* 2010;**44**:69–75.

Original Article

Isolation of Canine Coronary Sinus Musculature From the Atria by Radiofrequency Catheter Ablation Prevents Induction of Atrial Fibrillation

Hiroshi Morita, MD; Douglas P. Zipes, MD; Shiho T. Morita, MD; Jiashin Wu, PhD

Background—The junction between the coronary sinus (CS) musculature and both atria contributes to initiation of atrial tachyarrhythmias. The current study investigated the effects of CS isolation from the atria by radiofrequency catheter ablation on the induction and maintenance of atrial fibrillation (AF).

Methods and Results—Using an optical mapping system, we mapped action potentials at 256 surface sites in 17 isolated and arterially perfused canine atrial tissues containing the entire musculature of the CS, right atrial septum, posterior left atrium, left inferior pulmonary vein, and vein of Marshal. Rapid pacing from each site before and after addition of acetylcholine (0.5 μmol/L) was applied to induce AF. Epicardial radiofrequency catheter ablation at CS-atrial junctions isolated the CS from the atria. Rapid pacing induced sustained AF in all tissues after acetylcholine. Microreentry within the CS drove AF in 88% of preparations. Reentries associated with the vein of Marshall (29%), CS-atrial junctions (53%), right atrium (65%), and pulmonary vein (76%) (frequently with 2–4 simultaneous circuits) were additional drivers of AF. Radiofrequency catheter ablation eliminated AF in 13 tissues before acetylcholine ($P<0.01$) and in 5 tissues after acetylcholine. Radiofrequency catheter ablation also abbreviated the duration of AF in 12 tissues ($P<0.01$).

Conclusions—CS and its musculature developed unstable reentry and AF, which were prevented by isolation of CS musculature from atrial tissue. The results suggest that CS can be a substrate of recurrent AF in patients after pulmonary vein isolation and that CS isolation might help prevent recurrent AF. **(*Circ Arrhythm Electrophysiol.* 2014;7:1181-1188.)**

Key Words: atrial fibrillation ■ catheter ablation ■ coronary sinus ■ optical Vm mapping

Radiofrequency catheter ablation (RFCA) is a common treatment of atrial fibrillation (AF). The pulmonary veins (PVs) are frequent sources of AF, and thus are major targets of RFCA.[1] PVs contain muscular sleeves extending from the left atrial (LA) myocardium. Similar to PVs, the coronary sinus (CS) also has a muscular sleeve that connects the right atrium (RA) and LA.[2,3] Atrial tachyarrhythmias can arise spontaneously from the musculature of the CS[4,5] or after PV isolation by RFCA.[6,7] In some patients, macroreentrant atrial tachycardia (AT) in association with the CS[5] or by a focal atrial firing arising from the CS[6,7] initiates and drives AF. Thus, the CS is a possible ablation target to eliminate recurrent AF.[8–10]

Clinical Perspective on p 1188

The CS musculature can also be a source of triggered activity[11] and delayed conduction at the CS musculature and junctions between the CS and both atria. Such conduction delay also provides substrates for macroreentrant activity.[12–15] The vein of Marshall (VOM), which is a branch of the coronary veins connected to the LA and CS, is a substrate for reentrant circuit and foci of repetitive rapid responses.[16] Recently, we showed that muscular junctions between the CS musculature (including VOM) and both atria contributed to initiation of the atrial tachyarrhythmias by rapid pacing.[15] Rate-dependent conduction block in these pathways led to unstable reentry and AF-like activities.

Clinical and experimental observations indicate that isolation of the CS musculature from both atria by RFCA can be a secondary target for curing AF after completion of PV isolation.[8–10,15,17,18] In the current study, we investigated the relationship of the CS musculature to persistent AF induced by rapid atrial pacing with acetylcholine administration and the effects of CS isolation on the induction and maintenance of AF.

Methods

Arterially Perfused Atrial Tissue Preparations

The investigation conforms to the Guide for the Care and Use of Laboratory Animals published by the National Academy of Sciences (8th edition, Washington DC, 2011) and follows in accordance with our institutional guidelines. We prepared tissues with procedures similar to those used previously.[15]

Received February 12, 2014; accepted September 23, 2014.

From the Krannert Institute of Cardiology, Indiana University School of Medicine, Indianapolis (H.M., D.P.Z., S.T.M., J.W.); Department of Cardiovascular Therapeutics/Cardiovascular Medicine, Okayama University Graduate School of Medicine, Okayama, Japan (H.M., S.T.M.); and Department of Pharmaceutical Sciences, College of Pharmacy, Northeast Ohio Medical University, Rootstown (J.W.).

Correspondence to Hiroshi Morita, MD, Department of Cardiovascular Therapeutics, Okayama University Graduate School of Dentistry and Pharmaceutical Sciences, 2-5-1 Shikata-Cho, Okayama 700-8558, Japan. E-mail hmorita@cc.okayama-u.ac.jp

Circ Arrhythm Electrophysiol **is available at http://circep.ahajournals.org** **DOI: 10.1161/CIRCEP.114.001578**

We harvested hearts from 17 anesthetized adult male mongrel dogs and isolated atrial tissue preparations that contained the ostium of the CS (CSos), the CS musculature, the ligament of Marshall, the left inferior PV and lower interatrial septum of the RA, and the posterior LA from the posterior portion of the atrium and removed the free wall of the RA (Figure 1A). Each preparation contained the right coronary artery and the circumflex branch of the left coronary artery (diameter, ≈1–1.5 mm), into which separate perfusion and pressure monitoring cannulas were inserted. The tissues were mounted in a warmed chamber with epicardial surface in the focal plane of the mapping camera and were perfused with Tyrode's solution. Two silver electrodes were placed in the bath, 5 mm away from the LA (anode) and the RA (cathode) sides of the tissue, to register an ECG.[15]

The tissue preparations were stained with a voltage-sensitive fluorescent dye di-4-ANEPPS (Biotium, Inc, Hayward, CA, ≈4 mmol/L) and immobilized with cytochalasin D (Fermentek Ltd, Jerusalem, Israel, 20–30 μmol/L), which does not influence canine atrial action potentials (APs).[19] An optical mapping system with a 256-element (16×16) photodiode camera collected the fluorescence from a 33.6×33.6 mm^2 observation area on the tissue surface for general mapping and 19.5×19.5 mm^2 for detailed mapping of microreentry and converted it into 256 channels of electric signals. We recorded APs and ECG sequentially after 10 pacing stimuli at the cycle lengths (CLs) of 500 and 200 ms using a custom data acquisition system.[15]

The protocol for the experiments consisted of 5 parts and we examined all tissues during each part: (1) AF induction without acetylcholine, (2) AF induction with acetylcholine, (3) RFCA, (4) AF induction without acetylcholine after ablation, and (5) AT/AF induction with acetylcholine after ablation.

To induce atrial tachyarrhythmias, we paced the tissues with trains of 5 to 15 pacing stimuli, first at 180 ms CL and then repetitively with progressively abbreviated CLs in 10-ms steps until the occurrence of 2-to-1 conduction at each pacing site, including the CS, RA, LA, left inferior PV, and VOM. The above sequences of data recording were performed after tissue stabilization and verification (as the baseline control data) and then again after 10 minutes of stabilization after the addition of 0.5 μmol/L acetylcholine (Sigma-Aldrich, St. Louis, MO). Acetylcholine shortened AP duration and thus mimicked vagally induced AF in patients.[20]

We analyzed the shortest CL of 1:1 conduction at the CS, RA, LA, PV, and VOM, which indicated the longest refractory period in these pathways. We also analyzed the distributions of AP duration at the LA, RA, and the musculature of the CS during pacing CLs of 500 and 200 ms. We determined the muscular connections between the CSos-RA and CS-LA as reported previously.[2,3,15] For ease of reference, the proximal CS–LA (CSp–LA) junction was defined as the proximal or first half of the CS, whereas the distal CS–LA (CSd–LA) junction was defined as the distal or second half of the CS.

We analyzed conduction patterns of sustained (≥0.5 seconds) atrial tachyarrhythmias that were induced by rapid pacing from each site.[15] We defined AF as an atrial tachyarrhythmia with polymorphic changes of f waves in the ECG recorded between the RA and LA.[15]. Although there are no standard definitions of microreentry and macroreentry, we separated them by diameter of the reentrant circuit: macro >1 cm and micro ≤1 cm.

Radiofrequency Catheter Ablation to Isolate the CS

After induction of sustained atrial tachyarrhythmia with acetylcholine, we performed RFCA at the junctions between the CS musculature and both atria (Figure 1B) with a 4-mm tip catheter (Medtronic Conductor, Medtronic, Minneapolis, MN). Radiofrequency current (Atakr; Medtronic, Minneapolis, MN) was delivered between the catheter tip electrode and an Ag-Cl pad (1.5×1.5 cm^2) applied to edge of the tissue bath (5–10 W for 20–30 seconds; temperature ≤55°C).[21] We first applied RFCA energy around the CSos to isolate the CS musculature from the RA, and then performed linear ablation along the CSp–LA junctions. We evaluated the activation patterns during CS pacing after each ablation step. We additionally ablated the CSd–LA junction, if the LA was activated from the CSd–LA junction or from VOM after blockade of the CSp–LA junction. After isolating the CS from the atria, we evaluated the recurrence of conduction across the CS–atrial junctions for 20 minutes. Any remaining conduction between the CS and atria was then eliminated with additional RFCA. We repeated the pacing protocol to induce atrial tachyarrhythmias with and without acetylcholine after isolating the CS from the atria. To avoid excessive heat around the catheter, we superperfused the tissue at the ablation site with 60 mL/min Tyrode's solution (28–30°C) during RFCA.[21]

Statistics

Continuous data were expressed as mean±SD. Comparisons among mean values were performed with 2-way ANOVA coupled with Dunnett test. Comparisons of 2 groups were made with Student *t* test for unpaired data and paired data, as appropriate. We verified normality of the continuous data. Ordinal data were analyzed with Kruskal–Walis test. Fisher exact test was performed for the comparison of proportions among groups. Significance was defined as $P<0.05$.

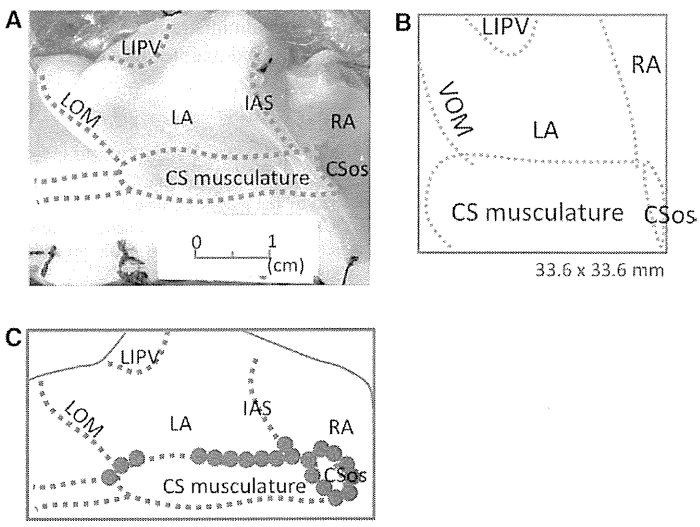

Figure 1. Tissue preparation and musculature of the coronary sinus. **A**, Posterior region of the atria that includes coronary sinus (CS). **B**, The epicardial area of 256-channel mapping usually covers the entire CS musculature, right atrial (RA) side of intra-atrial septum (IAS), left atrium (LA), left inferior pulmonary vein (LIPV), and vein of Marshall (VOM). **C**, Ablation points (red circles) electrically isolated CS from both atria in 3 steps: (1) circular ablation around ostium of CS (CSos), (2) linear ablation along the borderline between the CS musculature and LA, and (3) distal region of the CS in which VOM inserted to CS.

Results

Anatomy and Electrophysiological Properties of the CS Musculature

The visible CS musculature from the CSos to the distal end was 31±6 mm long and the diameter of the CSos orifice was 7±1 mm (Figure 1A). Muscular connections from the RA extended into the CSos and LA musculature directly to the CSp. The ligament of Marshall contained veins within the musculature that connected to the CS musculature in all tissues.

There were no statistical differences in AP duration and morphology between the LA, RA, PV, and CS musculature. Rapid pacing abbreviated the AP duration (Figure 2A). There were no statistical differences in the shortest pacing CL for 1:1 conduction among atrial sites (CS, 121±29 ms; RA, 124±25 ms; LA, 121±17 ms; PV, 123±18 ms; and VOM, 123±14 ms; P=0.9770), indicating similar longest refractory periods. Acetylcholine abbreviated AP duration at all sites. These data suggested similar electrophysiological properties among these muscular structures.

Induction of AF

At baseline, rapid pacing induced unstable macroreentry in association with conduction block at the CS–atrial junctions (Figures 3A and 4), resulting in AF-like ECG activity for 4.0±2.8 seconds (range, 1.5–12.0; median, 2.6 seconds). The average pacing CL that induced AF was 130±21 ms. LA pacing frequently induced AF, but the difference compared with other pacing sites did not reach statistical significance (incidence of induced AF: CS pacing 71%, RA pacing 77%, LA pacing 88%, and PV pacing 82%; P=0.6209). During AF, the RA had the longest mean CL of local activation among all atrial sites (Figure 2B). Unstable reentry usually appeared in association with the CS musculature and its atrial junctions, the VOM, PV, and intra-atrial septum (Figure 4), and usually 1 to 2 reentrant circuits existed simultaneously. During pacing-induced AF episodes at baseline, reentrant circuits were frequently associated with the CS musculature and the left inferior PV (Figure 2C).

After administration of acetylcholine, all tissues had sustained AF (>8 minutes) that either was induced by rapid pacing (pacing CL, 137±26 ms; n=14) or occurred spontaneously (n=3; Figure 3B). Because of the continuation of induced AF after acetylcholine, we could not evaluate 1:1 conduction systematically at all pacing and induction sites (induced pacing sites: 5 tissues at LA, 4 at PV, 4 at CS, and 1 at RA). Mean CL of local activation during AF with acetylcholine was shorter than at the baseline (Figure 2B). Compared with the RA and LA, CS and PV had shorter CLs of local activation during AF. AF after acetylcholine treatment had similar (usually 2–4 simultaneous) unstable reentrant circuits as the AF at the baseline and was associated more frequently with microreentry within the intra-atrial septum, PV and VOM (Figures 2C, 4C–4F, and 5) than with macroreentry between the CS and atria using CS–atrial junctions (Figures 4A and 4B). Moreover, microreentry within the CS musculature appeared frequently during AF after acetylcholine treatment (Figures 4F and 5). All AF episodes terminated spontaneously 2.3±1.7 minutes (median, 1.7 minutes) after acetylcholine washout.

CS Isolation From Both Atria

We isolated the CS with 3 RFCA steps and evaluated conduction during CS pacing. First, we performed circular ablation of the CSos (8.4±1.0 applications of RF energy) to block electric conduction between the CSos and RA (step 1, ablation of CSos–RA junction). Then a 13.8±7.5-mm linear ablation (range, 7–27; median, 12 mm) was performed (4.2±1.3 applications) along the CSp–LA junctions from CSp to CSd on the epicardium (step 2, ablation of CSp–LA junction). After step 2, connection between the CSd and LA was found in 12 tissues. These tissues subsequently received 2.9±1.1 applications RF energy to the CSd junction, resulting in 8.3±2.5-mm linear lesion (range, 5–14; median, 8 mm; step 3, ablation of CSd–LA junction; Figure 1B). The CSd–LA junction usually existed in association with branching of the VOM from the CS. We concluded that there was successful separation of the CSd–LA junction from the CSp–LA junction when their

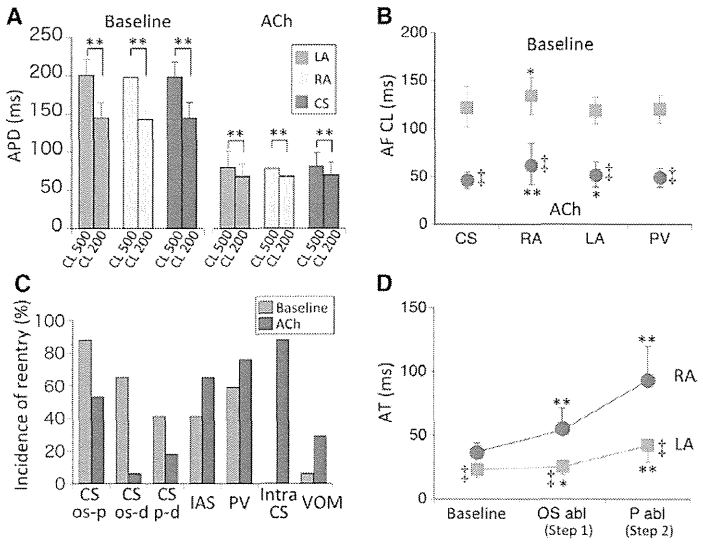

Figure 2. Action potential (AP) and its conduction in the atrium. **A**, AP duration (APD) in the left and right atria (LA and RA) and coronary sinus (CS). There were no statistical differences in APDs among the LA, RA, and CS. Short pacing cycle length (CL; 200 ms) abbreviated APDs. Acetylcholine (ACh) shortened APD at all sites. **P<0.01 vs CL=500 ms. ‡P<0.01. **B**, Mean CL during induced atrial fibrillation (AF) at each site. RA had the longest CL during AF at baseline. Acetylcholine abbreviated AF-CLs. AF-CLs were shorter in the CS and pulmonary vein (PV) than in the atria. **P<0.01 and *P<0.05 vs CS. ‡P<0.01 vs. baseline. **C**, Reentry. At baseline, reentry usually occurred in association with CS and its atrial junctions. Acetylcholine increased microreentry in the PV, intra-atrial septum (IAS), vein of Marshall (VOM), and CS. **D**, Activation times of the RA and LA during CS pacing. Ablation prolonged atrial tachycardias (ATs) in both atria. **P<0.01 vs control. ‡P<0.01 vs RA (N=17). Comparisons were performed with 2-way ANOVA coupled with Dunnett test (**A**, **B**, and **D**). OS abl indicates ablation at ostium of CS; and P abl, ablation at proxymal portion of CS.

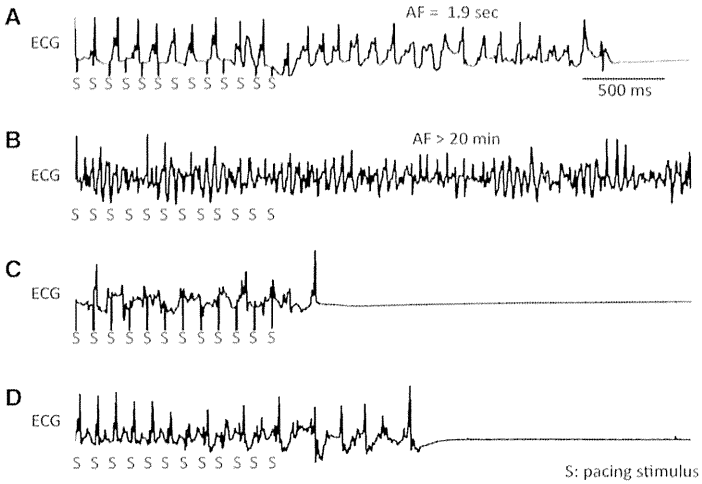

Figure 3. Atrial ECG characteristics of the induced atrial fibrillation (AF). **A**, Rapid pacing induced AF (duration: 1.9 s) at the baseline. **B**, After acetylcholine administration, rapid pacing induced sustained AF with finer waves than the baseline. **C**, After isolation of the coronary sinus (CS), rapid pacing induced only 1 to 2 echo beats. **D**, After isolation of the CS, administration of acetylcholine and rapid pacing induced short organized atrial tachycardia. Note these ECGs show atrial electrogram and do not include QRS complex.

ablation lines were ≥7 mm apart because single RFCA made a lesion of 3.8±0.9 mm diameter in these experiments.

Figures 2D and 6 show the changes in activation pattern in the RA and LA during CS pacing following each RFCA step. Before RFCA, excitation evoked by CS pacing propagated via the CS–atria junctions directly into both the RA and the LA (Figure 6A) with slightly earlier activation in the LA than in the RA (Figure 2D). After step 1 of RFCA, the RA was activated with significant delay via the interatrial septum (Figure 6B) from the LA, which was also delayed slightly. After step 2, the LA was activated from the CSd–LA junction. Both the LA and the RA activated significantly later than before step 2 (Figure 6C). Step 3 ablation fully isolated the CS, resulting in complete exit and entrance block (Figure 6D). Three tissues had reappearance of conduction at the CS–atrial junctions and required additional ablations to achieve electric isolation of the CS musculature.

Macroscopic observation after RFCA is shown in Figure 7. CS musculature connected directly to the LA at the upper side of the CS in CSp. Radiofrequency energy ablated the muscular connection of the CSp–LA junctions as well as the upper third of the CS musculature. At the CSd in which direct muscular connection was eliminated, small muscular bundles and VOM connected the CS and LA.

Effect of Isolation of CS Musculature From Both Atria on Induction of AF

We repeated electric stimulation after CS isolation. Although rapid pacing (CL, 132±22 ms) induced atrial tachyarrhythmias (≥0.5 seconds) in 4 tissues without acetylcholine, the duration of the tachyarrhythmias was significantly shorter than before RFCA (duration after RFCA, 0.4±0.8 seconds; range, 0–2.7 seconds; median, 0 second; $P<0.01$ versus before RFCA; Figure 3C). Short runs of reentrant tachycardia occurred in the interatrial septum (n=2) and left inferior PV (n=3).

Rapid pacing (CL, 128±18 ms) with acetylcholine induced atrial tachyarrhythmias (≥0.5 seconds) in 12 tissues. In contrast to the induced AF before RFCA, CS isolation organized the induced tachyarrhythmias into ATs having short durations (after CS isolation, 8.6±20.9 seconds; range, 0.9–81 seconds; median, 1.7 seconds; $P<0.01$ versus before RFCA; Figure 3D). Only 2 tissues had sustained AT (duration, 40 and 81 seconds, respectively) in association with the VOM and PV after RFCA. Residual reentry appeared in the left inferior PV (n=7; Figure 8A), intra-atrial septum (n=4; Figure 8B), and

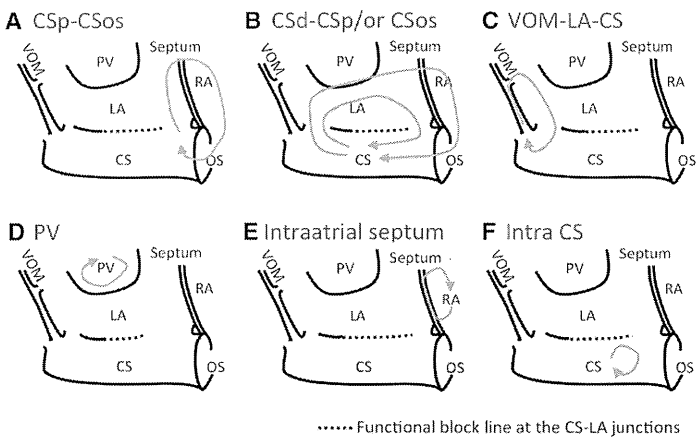

Figure 4. Schematic drawings of the unstable reentry induced by rapid pacing. **A**, Induced macroreentry of proximal coronary sinus (CSp)→left atrium (LA)→ right atrium (RA)→ostium of CS (CSos)→coronary sinus (CS)→CSp. **B**, Induced macroreentry of distal coronary sinus (CSd)→LA→RA→CSos/CSp→CS→CSd. **C**, Reentry of vein of Marshal (VOM)→LA→CSd→VOM. **D**, Microreentry associated with left inferior pulmonary vein (PV). **E**, Reentry associated with intra-atrial septum. **F**, Microreentry within the CS musculature. These reentrant circuits were usually unstable, resulting in atrial fibrillation–like ECG activity.

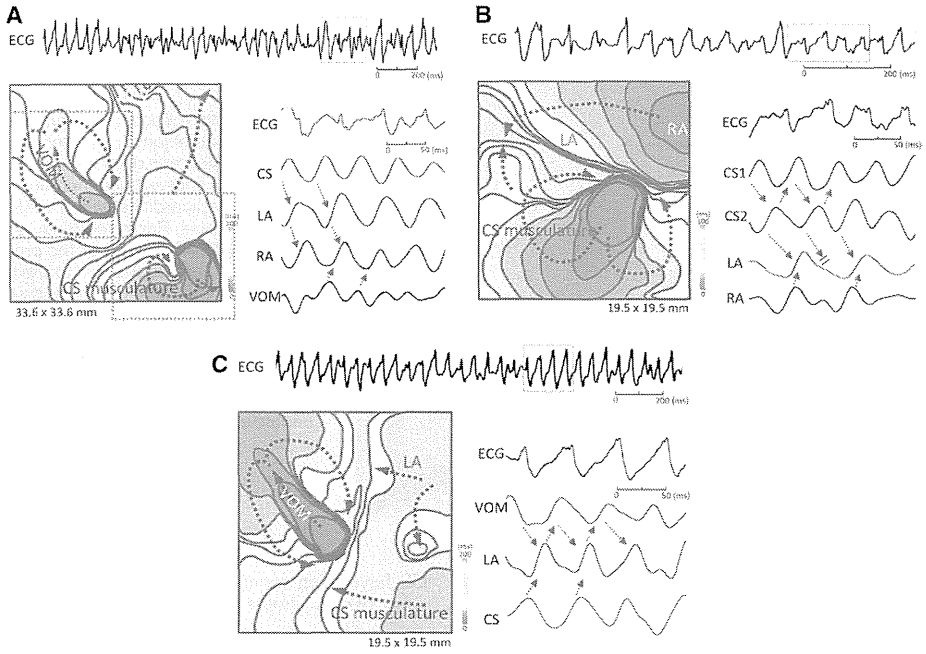

Figure 5. Microreentry during atrial fibrillation (AF) induced by rapid pacing and acetylcholine. **A**, Activation time map of the AF and action potentials. Activation time map showed that 2 microreentry appeared in the vein of Marshal (VOM) and coronary sinus (CS) simultaneously. **B**, CS was activated by rapid figure-of-8 microreentry and propagated 2:1 to the atria. **C**, VOM was activated from the proximal to distal and then propagated to left atrium (LA). Mapping area: 33.6×33.6 (**A**), 19.5×19.5 (**B** and **C**) mm². ECGs represent atrial electrogram and do not include QRS complex. RA indicates right atrium.

VOM (n=2; Figure 8C). Intra-CS reentry did not sustain for ≥0.5 seconds after CS isolation. Additional ablation to the residual reentrant circuits eliminated ATs in 9 tissues.

Discussion

We observed that rapid pacing–induced unstable macroreentry was associated with conduction slowing in the CS musculature and its atrial junctions, consistent with our previous findings.[15] New in this study, however, is that in addition to macrorentry, acetylcholine promoted microreentry involving the PV, VOM, and CS musculature and resulted in sustained AF. Importantly, microreentry within the CS musculature appeared only during AF induced by acetylcholine. Isolation of the CS musculature from both atria prevented induction of macroreentry in the CS musculature and organized AF into short-term ATs. Additional RFCA to the reentrant circuits associated with the ATs eliminated residual microreentry in the PV, VOM, and interatrial septum.

In addition to the initiation of AF from the PVs,[1] the musculature of the CS also has inherent arrhythmogenicity and can be a source of AT/AF.[3,5–11,13–15,17,22] The CS has been associated with initiation and maintenance of AF in 35% of patients

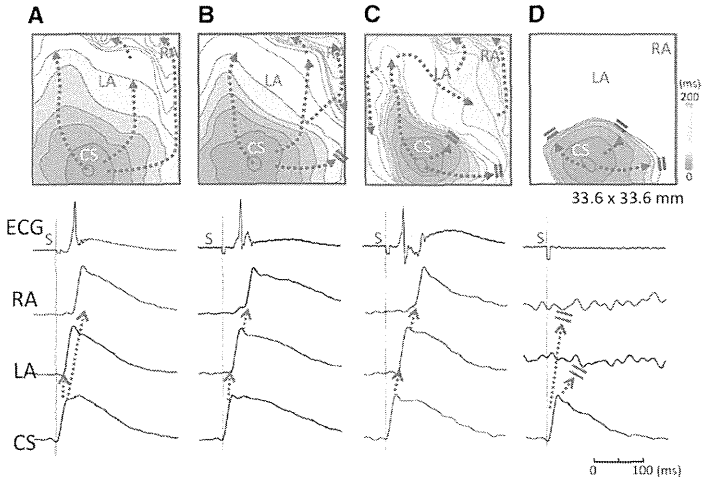

Figure 6. Activation of the atria during coronary sinus (CS) pacing before and after stepwise ablation. **A**, Atrial activation before ablation (ABL). Right atrium (RA) and CS were activated from ostium of CS (CSos) and proximal CS (CSp) junctions, respectively. **B**, Atrial activation after CSos-ABL. RA was activated from left atrium (LA) via CSp junction. **C**, Atrial activation after CSp-ABL. LA was activated from the distal CS (CSd; vein of Marshall) junction and then propagated to RA. **D**, Atrial activation after CS isolation. Activation during CS pacing did not propagate to both atria.